HYDROLOGIC IMPACTS OF CLIMATE AND LAND USE CHANGES IN THE WEST FORK SAN JACINTO RIVER OF TEXAS

A Thesis

by

JASON MICHAEL MURRAY

Submitted to the Office of Graduate and Professional Studies of
Texas A&M University
in partial fulfillment of the requirements for the degree of

MASTER OF SCIENCE

Chair of Committee,	Steven M. Quiring
Committee Members,	Huilin Gao
	Anthony T. Cahill
Head of Department,	David Cairns

August 2018

Major Subject: Water Management and Hydrological Science

ABSTRACT

Changes to climate and land use/land cover (LULC) are expected to be a source of uncertainty to streamflows in the Gulf Coastal Plains of Texas. Additionally, the city of Houston, Texas, is expected to experience spreading urbanization and immense population growth over the coming century, reaching 10 million people by 2050. As population grows over the next century so does the need for water in a city where groundwater is not a viable resource due to land subsidence. The West Fork San Jacinto (WFSJ) River's watershed is expected to undergo rapid urbanization as Houston continues to sprawl and the water supply reservoir located on the WFSJ River, Lake Conroe, will have an increased importance in the coming century.

Within the WFSJ watershed, changes in LULC are highlighted by an increase of urban land cover from 5.39% in 1992 to 14.7% in 2011. With this, impervious cover increased from 3.10% to 4.01% of the total watershed area from 2001 to 2011.

The WFSJ River's historical streamflow was investigated using two stream gauges for the periods of October 1974 to September 2016 and October 1984 to September 2016 for the upstream and downstream stream gauges, respectively. Historical trends for these periods were investigated using the Seasonal-Trend decomposition procedure based on Loess (STL), flow distribution, Richards-Baker Flashiness Index, and flow distribution. STL results showed a significant downward trend in streamflow for 3, 5, and 7 year trends. The only significant trend found was for mean monthly streamflow at both locations. This is possibly an indicator that urbanization had yet to reach a tipping point within the

watershed for the historical period, but may also indicate that streamflow data was inadequate for trend detection due to gaps in streamflow records.

The Variable Infiltration Capacity (VIC) hydrological model was utilized to investigate future scenarios of LULC and climate. A baseline period of 2001 to 2010 was established for climate and LULC and a future period was set for 2080 to 2089. Future climate scenario was based on the Representative Concentration Pathway 8.5 (RCP8.5) and future LULC was based on the USGS LandCarbon A2 scenario. In total, four scenarios were ran using VIC: baseline, LULC change, climate change, and combined LULC and climate change. Under the LULC change scenario streamflows increased by 0.39% and 4.66% for spring and summer, respectively, but decreased by 0.64% and 6.76% for fall and winter, respectively. Under the climate change scenario, streamflows decreased by 38.96%, 56.79%, 76.06%, and 48.44% for winter, spring, summer, and fall, respectively. The combined LULC and climate change scenario also exhibited decreases by 34.75%, 44.31%, 68.90%, and 45.12% for winter, spring, summer, and fall, respectively.

Decreases in precipitation and increases to temperatures associated with climate change create an environment that favors lower streamflows but LULC changes have the ability to counteract these decreases. The study highlighted the uncertainty facing the water resources of the WFSJ watershed and Lake Conroe. The results indicate that less water will be available for the growing Houston metropolitan area.

CONTRIBUTORS AND FUNDING SOURCES

This work was supervised by a thesis committee consisting of Dr. Steven Quiring [Committee Chair] of the Geography Department and Dr. Huilin Gao [Committee Member] and Dr. Tony Cahill [Committee Member] of the Civil Engineering Department.

There are no outside funding contributions to acknowledge related to the research and compilation of this document. All work for this thesis was completed by the student.

TABLE OF CONTENTS

LIST OF FIGURES

Page

LIST OF TABLES

1. INTRODUCTION

1.1 Problem Statement

Uncertainty in future streamflows and extreme weather events threaten the water resources and infrastructure that are necessary for normal everyday life. Due to the complicated nature of hydrologic modeling and disconnects between scientists and decision makers, there is little known about the effects of changes in climate and land use on the hydrology of watersheds in the Gulf Coastal Plains (GCP) of Texas (Bates et al., 2008).

The city of Houston experienced immense growth from 2000-2010 and reached ~6 million people. If the growth rate remains the same, by 2050 the population of Houston's metropolitan area is expected to reach 10 million (Demographer, 2014). This population growth stresses water resources and an aging infrastructure. Exacerbating this problem is the threat of climate change which brings with it the increased potential and probability of problems from flooding as well drought. Thus, as the need for domestic water supply is growing, it is simultaneously being threatened by climate change.

Another factor impacting the sustainability of the Houston metropolitan area is that areas were subjected to land subsidence due to aquifer compaction from groundwater pumping. The irreversible compaction of these areas have increased flood risk and resulted in loss of established wetland area (Ingebritsen and Galloway, 2014). The potential for loss of life and costly damage to infrastructure or property highlights the need for better decision making and an increase in studies on the region to arm these decision makers with the best possible knowledge. Thus, the purpose of this thesis is to provide decision

makers with an additional source of knowledge towards planning and management of water resources faced with uncertainty of seasonal and annual water quantity.

1.2 Hydrologic Response to Climate Change

There are many differences between watersheds, as well as many different possible scenarios of climate change that are based upon differing human activities in the future. For this reason, the Intergovernmental Panel on Climate Change (IPCC) has published reports and syntheses concerning climate change based upon the working groups of the IPCC. In these reports an array of climate model scenario outputs are presented in which projections about the future climate are made based on land use as well as greenhouse gas (GHG) and air pollution emissions (Pachauri et al., 2014). The magnitude of which these factors are determined by the IPCC is determinate upon projections of technological advances, human behavior and population growth and as a result they present several scenarios that range from no climate change to extreme climate change.

These IPCC scenarios have been utilized to simulate through models the impacts of climate change on hydrological processes to predict future changes in watersheds around the world. For example, the Tibetan Plateau's hydrology under IPCC climate scenarios A1B, A2, and B1 was simulated using the Variable Infiltration Capacity (VIC) hydrologic model (Liu et al., 2015). The authors found that reductions in streamflow are to be expected for spring and summer while annual precipitation and runoff increases coupled with a dramatic decrease in snow cover. In a similar study that utilized the IPCC scenarios it was found that a 10% decrease in rainfall resulted in a 30% decrease in

discharge and a 1.5°C decrease in temperature accounted for a 15% reduction in discharge of a tropical watershed in Ethiopia, Africa (Legesse et al., 2003).

The importance of these findings on the effects of climate change can be exemplified by a study on the hydrology of the Columbia River basin. It was shown that an increase in winter streamflow is expected, while spring and summer streamflow reductions by 2045, which would negatively impact irrigation, hydro-power, recreation, and instream fish (Hamlet and Lettenmaier, 1999). This study by Hamlet and Lettenmaier (1999) also showed that it could be expected that reductions in winter snow pack would result in the river system no longer being a snow-melt dominated system. These potential negative impacts on water resources are supported by another study on the Colorado River for the years 2010-2100 which found that under future climate scenarios mandated Glen Canyon Dam releases were only met in 59-75 percent of years and a reduction of annual hydropower production between 45 and 56 percent (Christensen et al., 2004).

The seasonal patterns of precipitation and evapotranspiration within the Gulf Coast region of the U.S., results in stresses on water resources, and these are expected to be exacerbated by climate change (Mulholland et al., 1997). An important question is how will water resources be affected by climate change. Olivera and DeFee (2007) found that changes in precipitation from 1970-2000 accounted for 39 percent of the annual runoff increase and 96 percent of the annual peak flow increase in the Whiteoak Bayou in Houston (Olivera and DeFee, 2007). This illustrates that changes in precipitation patterns can have large a large impact on runoff in this region.

Regional studies have estimated that the number of precipitation events within the GCP of Texas is expected to decrease, but intensity of these events are expected to increase by ~20-30 percent between 2020-2099 based on moderate climate change scenarios (Biasutti et al., 2012). Tropical cyclones are a relatively common occurrence in this region and they often cause significant rainfall. Climate change is expected to increase precipitation rates by ~20% and cyclone intensity by ~11% (Knutson et al., 2010). This will also have a direct impact on future patterns of runoff and flooding. Zhu et al. (2015), for example, found that tropical cyclones accounted for 20% of the high flow events in four watersheds near Houston and the watersheds with more intense urbanization had greater extreme flows. The probability of extreme rainfall from hurricanes of 500 mm was about 1% for the period of 1981 to 2000 and will increase to 18% for the period of 2081 to 2100 (Emanuel, 2017).

These findings reinforce that high intensity precipitation events are likely to become more common in the future. As a result, stream flow is expected to become more variable in the future and this will create higher variability in reservoir levels (Muttiah and Wurbs, 2002). This is primarily a problem in low capacity reservoirs because reservoirs with a greater storage capacity are better equipped to handle sudden influxes of runoff (Muttiah and Wurbs, 2002).

1.3 Hydrologic Response to Land Cover Changes

The relationship between changes in land cover and changes in streamflow has been well studied. One of the predominant characteristics of urbanization is the increase of impervious cover. The increase in impervious surfaces has been shown to decrease lag

time between the onset of precipitation events and peak streamflow with an increase in peak streamflow and total runoff volume (Shuster et al., 2005). Impervious cover reduces the ability of water to infiltrate the surface and creates a greater percentage of incoming precipitation becoming direct runoff. Increases in impervious cover lead to increased likelihood and severity of flooding downstream of urbanized areas (Michener and Haeuber, 1998). Once impervious cover is greater than about 10%, this has been shown to increase peak flows such that what was previously a 10-year flood event becomes a 2-year flood event (Booth, 2000).

An additional consequence of urbanization is the decrease of base flow (Meyer, 2005; Pluhowski and Spinello, 1978). Base flows are controlled by a complex network of surface and subsurface pathways. These pathways can be greatly altered by urbanization (Price, 2011). Specifically, more precipitation becomes direct runoff rather than infiltrating the soil. Under natural conditions, this water would enter sub-surface systems of which a portion would eventually be released into streams in a longer timeframe. Additionally, the increased evaporation in urban areas results in a greater portion of water never reaching the stream network.

A study of streamflow in the Weihe River Basin of China found that human activities in during the 1970s to the 2000s had an accounted for 60 percent of experienced changes in streamflow while climate change had an average impact of 34 percent (Chang et al., 2015). The authors concluded that human activities such as artificial withdrawals, land cover changes, and diversions of water in the river basin exacerbated the reductions of precipitation. This illustrates that human activity can alter the hydrology of a watershed

and that both future land cover change and climate change should be considered in future water resources planning.

While results of studies on climate or land cover changes on a watershed provide useful information, there is added value to observing the effects of both. By the year 2050, the impacts of climate and land cover change in the Lower Virgin River are expected to result in a slight increase of summer streamflow while in the winter months it is expected to see a decrease in streamflow of 34.8% to 75.4% (Chen et al., 2015). The authors of this study also found that climate change is expected to have a greater effect on the streamflow than land cover. This study compared with Hamlet and Lettenmaier's (1999) study illustrates that while both watersheds are expected to be primarily influenced by climate change they are also expected to have different changes and magnitude of changes as a result.

Houston has been experiencing rapid urbanization. Impervious surfaces in Houston increased by 21% from 1984-1994, 39% from 1994-2000, and 114% from 2000-2003. As a result, the median rainfall-runoff ratio within Houston watersheds increased by 24% (Khan, 2005). Olivera and DeFee (2007) also found that impervious cover was responsible for 77% of the increase in annual runoff volume and 32% of the increase in annual peak flows from 1949-2000. Similarly, a retrospective study found that catchment imperviousness increased from 15% in 1990 to 17% in 2000 which caused an increase in extreme peak flows and an increase in households being flooded by 100-year flood events in Sims Bayou in Houston, TX (Muñoz et al., 2017).

Other changes in land cover can also influence watershed hydrology. For example, naturally occurring wetlands have been shown to decrease the amount of damage from flooding events (Brody et al., 2014; Brody et al., 2007b; Highfield and Brody, 2006). These wetlands are often disturbed in rapidly urbanizing and suburbanizing watersheds, such as those of Houston, which have been linked to exacerbated flooding events (Brody et al., 2007a).

1.4 Sustainability and Resilience

Given the uncertainties about how changes in climate and land use will impact watershed hydrology, there is a great need for sustainable development and management of water resources. There is a need for a decision framework that balances the ecological and economic interests for the design and implementation of infrastructure (Poff et al., 2016). Studies that utilize climate change scenarios and land use trends can provide valuable insight for decision makers and stakeholders into how the watersheds and water resources are expected to change. These studies, as mentioned by Hossain et al. (2015), provide valuable input for Poff et al.'s (2016) decision frameworks towards planning resilient water infrastructure.

Water infrastructure in many locations of the United States has not been properly maintained and so as it ages, it becomes more susceptible to extreme weather (Hossain et al., 2015). Hossain et al. (2015) noted that even when upgrades occur, they may not be successful because they do not account for potential future changes in precipitation and land use. This can be seen in studies that simulate impacts due to changes in land cover as

well as climate (Chang et al., 2015; Chen et al., 2015; Legesse et al., 2003; Mango et al., 2011).

The need for resilience is especially important in watersheds that have water intensive industrialization. Industry is particularly in need of resilience for water resources as illustrated by the Dow Chemical Company of Freeport, Texas who during times of drought may have increased water supply costs and shortages. The company utilized the VIC model to run climate scenarios and a hydro-economic model to strategically plan for the uncertainties in future water resource shortages (Reddy et al., 2015). This strategic planning of their usage of water resources prevented losses during times of increased water prices due to forecasting economic risks due to predicted of water supply shortages. This case study provides important support for the ideas of Poff et al. (2016) and Hossain et al. (2015) towards the need and value of the planning and development of resilient water resources.

With the increased risks of flooding in the greater Houston area there is also an increased need for studies that provide information for decision makers. From 1984 to 2003 the prevalence of urbanization has been correlated with an increase in runoff at most stream gauges in the area (Khan, 2005). However, there has been very few publications about what is to be expected based on land cover change and climate change in the region. Mango et al. (2011) explains that any modelling effort requires an understanding of the system they are modeling.

1.5 Research Objectives

This thesis will quantify how the expected changes in land cover and climate within the GCP of Texas will impact the hydrology of the West Fork of the San Jacinto River. The primary research objectives are to: (a) describe historical patterns and trends in annual and seasonal streamflow, (b) quantify expected changes in urban land use from 2010 to 2090 in the West Fork San Jacinto watershed, and (c) model how projected changes in climate and land use will influence annual and seasonal streamflow.

2. METHODS

2.1 Study Area

The study area is the West Fork San Jacinto (WFSJ) River which is located north of Houston, Texas (Figure 1). The WFSJ Watershed has a total drainage area of 2,802 km^2. The drainage area above the USGS stream gauge 8068090 is 2,550 km^2. This watershed was selected due to it being within the GCP which is located on the southern shores of the United States with the Gulf of Mexico. Additionally, with the proximity to Houston the watershed is an area of active urbanization.

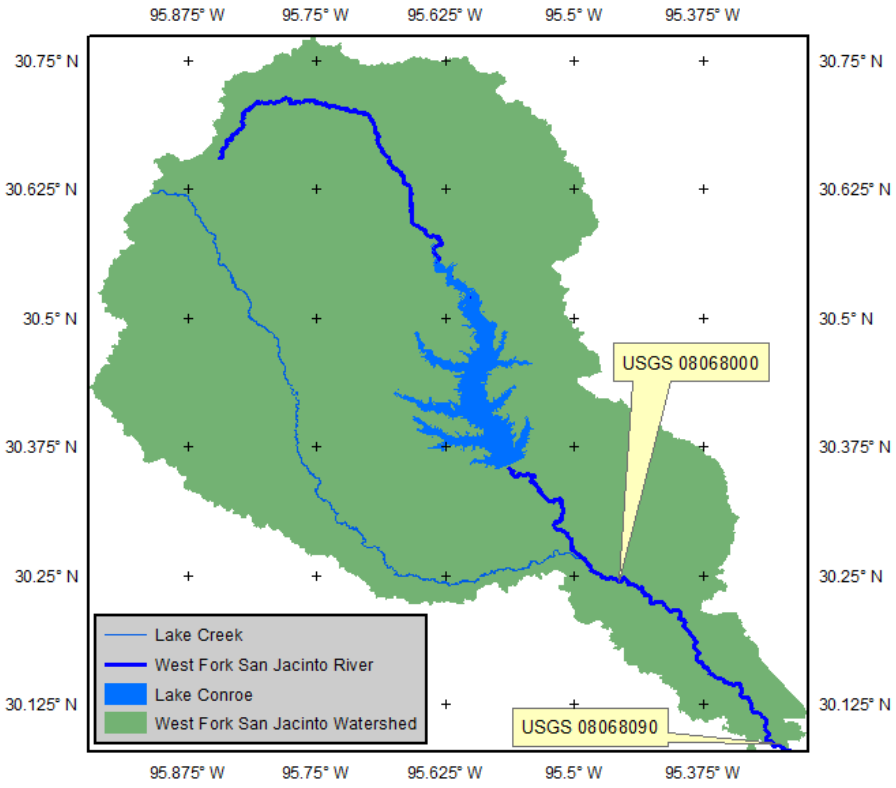

Figure 1. West Fork San Jacinto River and watershed.

Urban areas in this region have experienced serious flooding events in recent years. For example, in 2015 flooding in Houston, Texas resulted in damages of more than 3 billion U.S. dollars (Baddour, 2015). Then in September 2019, Hurricane Harvey, a category 4 hurricane, made landfall near Rockport, TX and caused about 126 billion U.S. dollars of damage from historic flooding (SOURCE). Drought risks are also of concern for the Southern United States as climate change is expected to reduce summer and winter precipitation for the region (Hyndman, 2014).

Water resource managers face uncertainty because future land use changes and climate changes both may lead to substantial changes in runoff. The increase in impervious surfaces that characterize urbanization are one of the major land use changes that influence runoff patterns. The US Census Bureau identified Houston as one of the most sprawling cities in the United States. It has a high population, but a relatively low population density as compared to other cities of similar population.

Lake Conroe is located within the WFSJ watershed. It is an important water supply and recreational reservoir for the Greater Houston Area. Construction of Lake Conroe was completed in January 1973 and it was filled in October 1973. The lake has a surface area of ~8.9 km^2, a storage capacity of 530,720,000 m^3, an average depth of 6.1 meters, a maximum depth of ~21.3 m, a length of ~41.8 km, and a width of ~9.7 km.

2.2 Data

2.2.1 Streamflow Data

Streamflow data for the WFSJR is available from the United States Geological Survey (USGS) stream gauges 08068000 and 08068090. These data are available as

average daily, monthly, and yearly streamflows. The period of records for the stream gauges are shown in Tables 1 & 2. Stream gauge 08068090 has a gap of data from 1995-09-30 to 2001-09-29.

Table 1. USGS stream gauge 08068000 data summary.

W Fk San Jacinto near Conroe, TX - USGS 08068000		
Data	Period of Record	
	Begin	End
Mean Daily Discharge	1974-10-01	2016-09-30
Mean Monthly Discharge	1974-10	2016-09
Mean Annual Discharge	1974	2016
Peak streamflow	1974	2016

Table 2. USGS stream gauge 08068090 data summary.

W Fk San Jacinto Rv abv Lk Houston nr Porter, TX - USGS 08068090		
Data	Period of Record	
	Begin	End
Mean Daily Discharge	1984-10-01	2016-09-30
Mean Monthly Discharge	1984-10	2016-09
Mean Annual Discharge	1984	2016
Peak streamflow	1984	2016

2.2.2 Meteorological Data

Gridded daily precipitation (mm), minimum temperature (°C), maximum temperature (°C), and average 10-m wind speed (m/s) were obtained for the time period of 1949-2010 from Maurer et al. (2002). The original dataset was for the period of 1949-2000, but it was updated in 2013 to include data through 31 December 2010. These data are gridded to $1/8^{th}$ degree (~140 km^2) grid cells, shown in Figure 2, and they are based on meteorological measurements from stations across the conterminous North America.

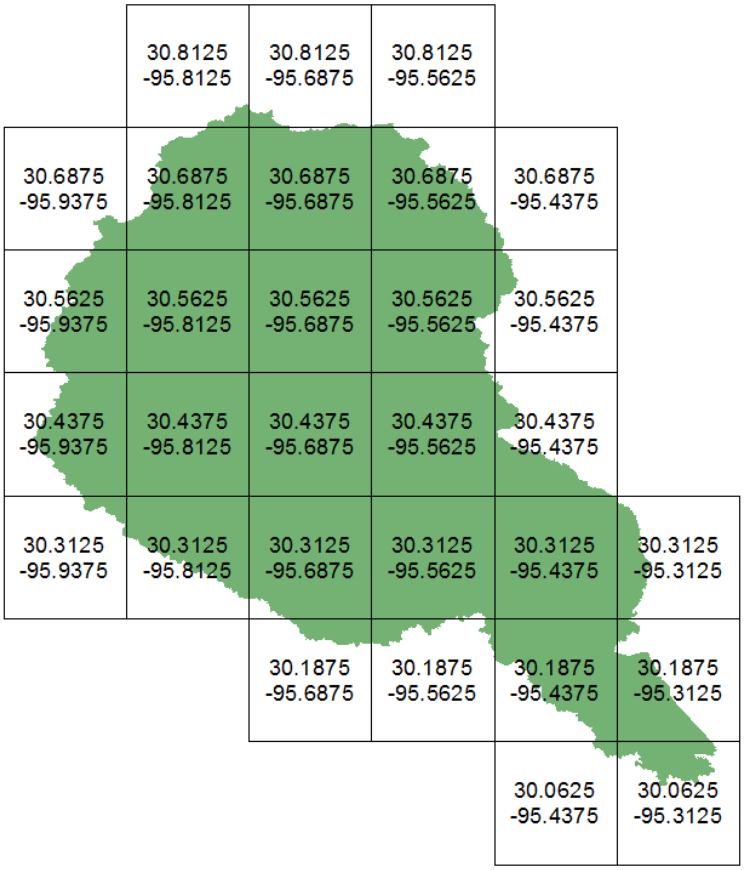

Figure 2. Map of grid cells used from the Maurer et. al. (2002) dataset.

2.2.3 Land Cover Data

Land cover data from the 0.5 km MODIS-based Global Land Cover Climatology (GLCC) data were obtained from the USGS Land Cover Institute website (Broxton et al., 2014; Channan et al., 2014; Friedl et al., 2010). The GLCC dataset is an improvement of the MODIS land cover type data product (MCD12Q) classification for the time period of 2001-2010. Broxton et al. (2014) found that the single-year land covers in the MCD12Q dataset gave unreasonable land cover changes from year to year due to difficulties in the

algorithm identifying similar land cover types. Thus, they created the GLCC dataset to reduce errors by weighting land cover types per year based on confidence scores to better represent the spatial distribution of land cover types while maintaining the frequency of land cover types.

Percent developed imperviousness (PDI) and land use/land cover (LULC) data were also obtained from the National Land Cover Database (NLCD) which is hosted on the Multi-Resolution Land Characteristics Consortium's website (Fry, 2011; Homer et al., 2007; Homer et al., 2015; Vogelmann et al., 2001). Both the NLCD PDI and LULC data has a 30 m resolution. Each cell within the PDI dataset contains an integer value that represents the percent of land within the cell that is PDI. The LULC dataset has coded values that are representative of their LULC classification.

2.3 Historical Streamflow and Land Use/Land Cover Analysis

2.3.1 Historical Streamflow Analysis

The Seasonal-Trend decomposition procedure based on Loess (STL) was utilized to identify trends in streamflow (Cleveland et al., 1990). The STL method has long been a popular choice for analyzing trends and has been successfully applied to analyzing and de-seasonalizing streamflows (Adnan et al., 2017; Lall, 1995). The period analyzed for stream gauge 08068000 was from October 1974 to September 2016. Due to the data gap with stream gauge 08068090, the periods analyzed were from October 1984 to August 1996 and October 2001 to September 2016.

Streamflow percentiles were calculated using the streamflow data following the construction and filling of Lake Conroe. Additionally the flow distribution, daily

streamflow variation, and high flow frequency were calculated. Flow distribution (T_{qmean}) is represented by the fraction of time that flow exceeds the mean flow, calculated according to Konrad and Booth (2005) as:

$$T_{qmean} = \frac{\#\ Days\ greater\ than\ mean\ streamflow}{\#\ Days\ in\ year}$$

Daily streamflow variation is explained by the Richards-Baker Flashiness Index (R-B Index) which was calculated according to Baker et al. (2004) as:

$$R - B\ Index = \frac{\sum_{i=1}^{n} |q_i - q_{i-1}|}{\sum_{i=1}^{n} q_i}$$

where q_i is the daily discharge at day i, n is the number of days in a year. A higher R-B Index indicates a higher amount of daily variation.

Lastly, high flow frequency is explained as being the number of occurrences in a year of streamflow being greater than three times the median streamflow (Clausen and Biggs, 2000).

2.3.2 Land Use/Land Cover Change Analysis

To identify changes in land use/land cover for the period of 1992-2011 the Spatial Analyst extension in ArcGIS was utilized in conjunction with the NLCD 1992, 2001, 2006, and 2011. Areas of each land cover class was calculated within the WFSJ watershed boundaries then converted to percent coverages for comparison.

The NLCD 1992 data were completed using a different methodology than the 2001, 2006, and 2011 data with different land cover classes. Thus, the classifications were combined into simplified land cover classes (Table 3). The MRLC advises against direct comparison of the NLCD 1992 data with the NLCD 2001-2011 data. Thus, the comparison

of the 1992 data with the 2001 data is taken with a grain of salt and conclusions was not formulated upon it and it was only considered in a qualitative manner.

Table 3. Simplification table for the NLCD classes.

Simlified NLCD	NLCD 1992	NLCD 2001-2011
Open Water	11 - Open Water	11 - Open Water
Developed	21 - Low Intensity Residential	21 - Developed, Open Space
	22 - High Intensity Residential	22 - Developed, Low Intensity
	23 - Commercial/Industrial/Transport	23 - Developed, Medium Intensity
	31 - Bare Rock/Sand/Clay	24 - Developed, High Intensity
	32 - Quarries/Strip Mines/Gravel Pits	31 - Barren Land
	85 - Urban/Recreational Grasses	
	33 - Transitional	
Forested	41 - Deciduous Forest	41 - Deciduous Forest
	42 - Evergreen Forest	42 - Evergreen Forest
	43 - Mixed Forest	43 - Mixed Forest
Agricultural	71 - Grasslands/Herbaceous	52 - Shrub/Scrub
	81 - Hay/Pasture	71 - Grassland/Herbaceous
	82 - Row Crops	81 - Hay/Pasture
		82 - Cultivated Crop
Wetland	91 - Woody Wetland	90 - Woody Wetland
	92 - Emergent Herbaceous Wetland	95 - Emergent Herbaceous Wetland

2.4 VIC Model

The Variable Infiltration Capacity (VIC) Model is a macroscale hydrologic model which solves water and energy balances over individual grid cells (Liang et al., 1994; Liang et al., 1996). The VIC model allows for sub-grid heterogeneity through statistical distribution. This is what separates the VIC model from other hydrologic models as parameters for soil, vegetation, and topography are represented spatially compared to other models where all parameters are typically averaged across entire catchments.

The basic model inputs are broken into the global parameters, the meteorological forcings, soil parameters, vegetation parameters, and vegetation library files. The global

parameters file is the primary input file and tells the VIC model where other input files may be found and the formatting of what they contain.

2.4.1 Meteorological Forcing Files

Meteorological forcing files from Maurer et al. (2002) were used. These data include daily precipitation (mm), minimum and maximum temperature (°C), and average 10-m wind speed (m/s). These data are gridded at a $1/8^{th}$ degree resolution (~12 km). Each grid cell is represented by a single tab separated ASCII text file that spans from 1949-2010.

2.4.2 Soil Parameter File

Soil parameters from Maurer et al. (2002) were used. The soil parameter file defines the $1/8^{th}$ degree grid cells geographic location and their grid cell ID, shown in Figure 3, which is used to link with the meteorological forcing files and vegetation parameters file. The soil parameter file also contains variables that define the thermal and hydrologic parameters of each grid cell.

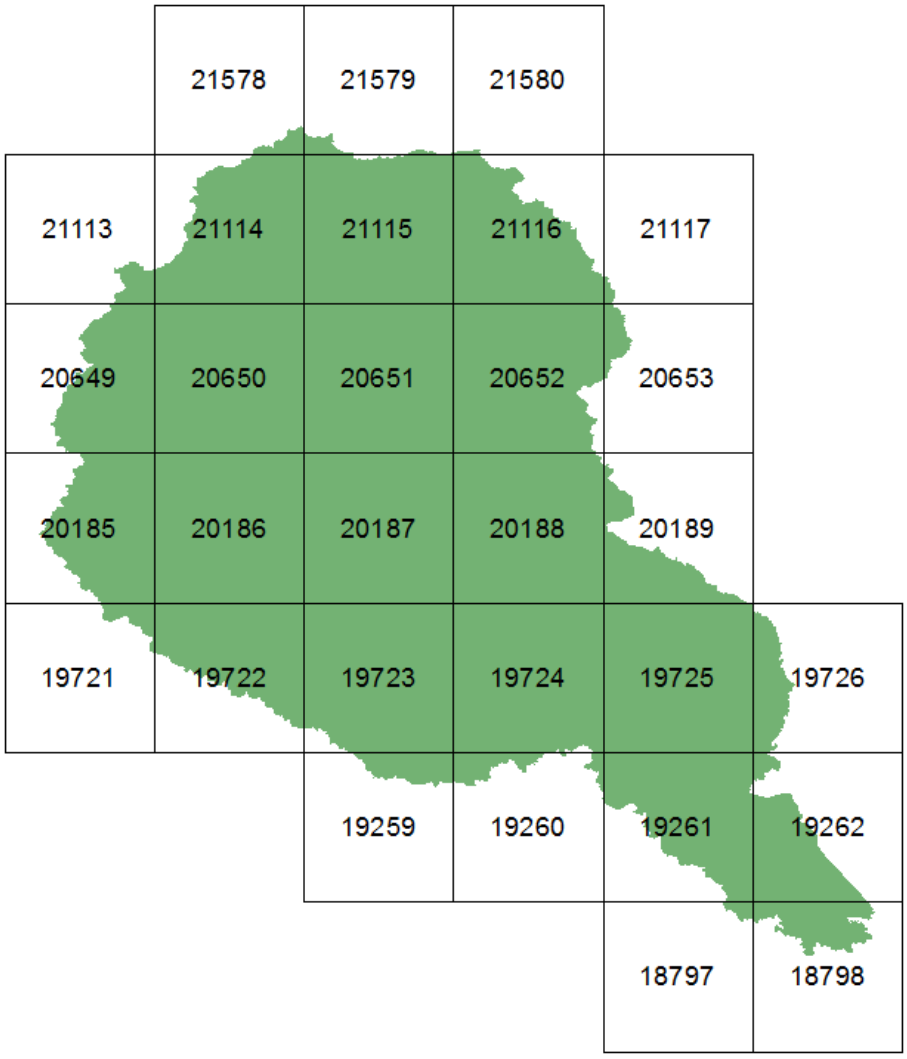

Figure 3. Map of soil grid cells and their ID used in this study.

2.4.3 Vegetation Library File

The vegetation library file from Maurer et al. (2002) was used. The vegetation library file defines available land cover types and provides the vegetation parameters associated with them. Modifications were made to the vegetation library file to include the urban land cover which was previously not included. The vegetation parameters of the

urban land cover are based on turf grass and it is assumed that the grass covers 50% of the land cover class. The other 50% is recognized by the model as bare soil which is used to represent developed surfaces. The classes of the library file are shown in Table 4.

Table 4. Vegetation library file classes.

Class #	Class Name
1	Evergreen Needleleaf
2	Evergreen Broadleaf
3	Deciduous Needleleaf
4	Deciduous Broadleaf
5	Mixed Cover
6	Woodland
7	Wooded Grasslands
8	Closed Shrublands
9	Open Shrublands
10	Grasslands
11	Crop land (corn)
12	Urbanized

2.4.4 Vegetation Parameter File

The vegetation parameter file defines the classes within the grid cell and the fraction of their coverage within those grid cells. The vegetation parameter file from Maurer et al. (2002) was used for the parameter values it defines, however the subgrid heterogeneity was resampled with higher resolution GLCC data. Urban land cover types are typically underrepresented, or completely disregarded, due to difficulties associated with identifying urban and built-up land cover types. For this reason the NLCD 2011 Percent Developed Imperviousness (PDI) cover dataset was used to identify additional cells where urbanization is pronounced. The 30 m PDI data was used to create a 0.5 km grid of PDI based on averages within the cells. The resulting grid was used to reclassify cells of the GLCC dataset based on a PDI of 30% or greater as the urbanized land cover.

The original version of the Maurer et al. (2002) vegetation parameters and library is based on the classes of the 1 km resolution University of Maryland (UMD) Global Land Cover Classification (Hansen et al., 2000). However, the MODIS-based GLCC provides a better representation of urban and other less dominant land covers that are typically underrepresented at coarser resolutions.

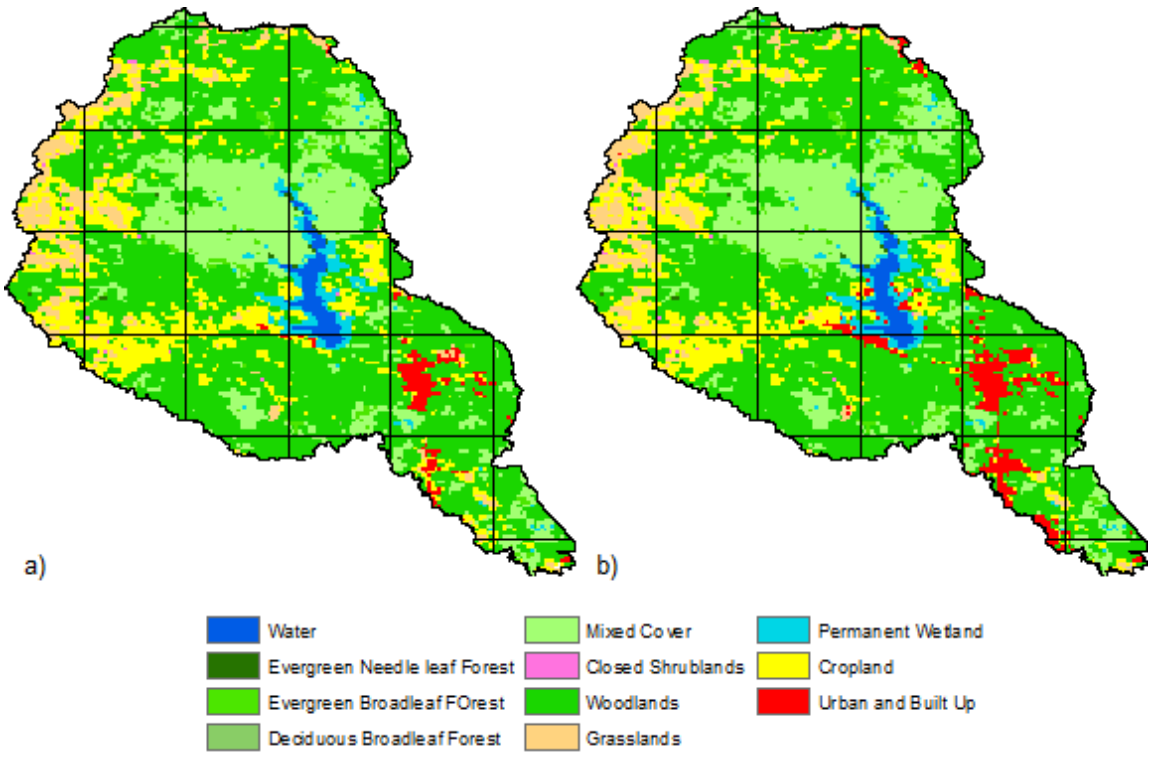

Figure 4. Map of land cover within the watershed based on a) pre-existing GLCC data and b) re-sampled urban land cover based on NLCD's PDI dataset.

The GLCC land cover classifications were translated to the VIC vegetation classes as show in Table 5. The land cover fractions were recalculated for all grid cells using the Spatial Analyst extension of ArcGIS (Figure 4). Only areas within the watershed were considered for calculating the land cover within each grid cell as shown in Figure 5. Permanent wetland, barren or sparsely vegetated, and water GLCC classes were removed.

The remaining values were then equally filled so the sum of sub grid class fractions equaled 1.

To account for the hydrologic impact of Lake Conroe on the watershed, the optional lake parameter file was utilized (Bowling and Lettenmaier, 2010; Gao et al., 2011). Lake bottom elevation data from the Texas Water Development Board was used to create the necessary lake depth profile by converting the points into a raster, reclassifying the data into 11 equal intervals, then calculating the percent coverage of each interval for the respective grid cell (Solis et al., 2012).

Table 5. Comparison of GLCC and UMD land cover classifications. Adapted from Friedl et al. (2010).

Vegetation group	GLCC	UMD	VIC Vegetation
Forests	Evergreen needleaf forest	Evergreen needleaf forest	Evergreen needleaf forest
	Deciduous needleleaf forest	Deciduous needleaf forest	Deciduous needleaf forest
	Evergreen broadleaf forest	Evergreen broadleaf forest	Evergreen broadleaf forest
	Deciduous needleleaf forest	Deciduous broadleaf forest	Deciduous broadleaf forest
	Mixed forests	Mixed forests	Mixed Cover
Woodlands	Woody savannas	Woody Savannas	Woodland
	Savannas	Savannas	Woodland
Grasses	Grasslands	Grassland	Grasslands
Shrublands	Closed shrublands	Closed shrublands	Closed shrublands
	Open shrublands	Open shrublands	Open shrublands
Croplands	Croplands	Croplands	Croplands
	Cropland/natural vegetation		Croplands
Inundated	Permanent wetland		N/A
Unvegetated	Urban and built-up land	Urban and built-up land	Urban and built-up land
	Barren or sparsely vegetated	Barren or sparsely vegetated	N/A
	Water	Water	N/A

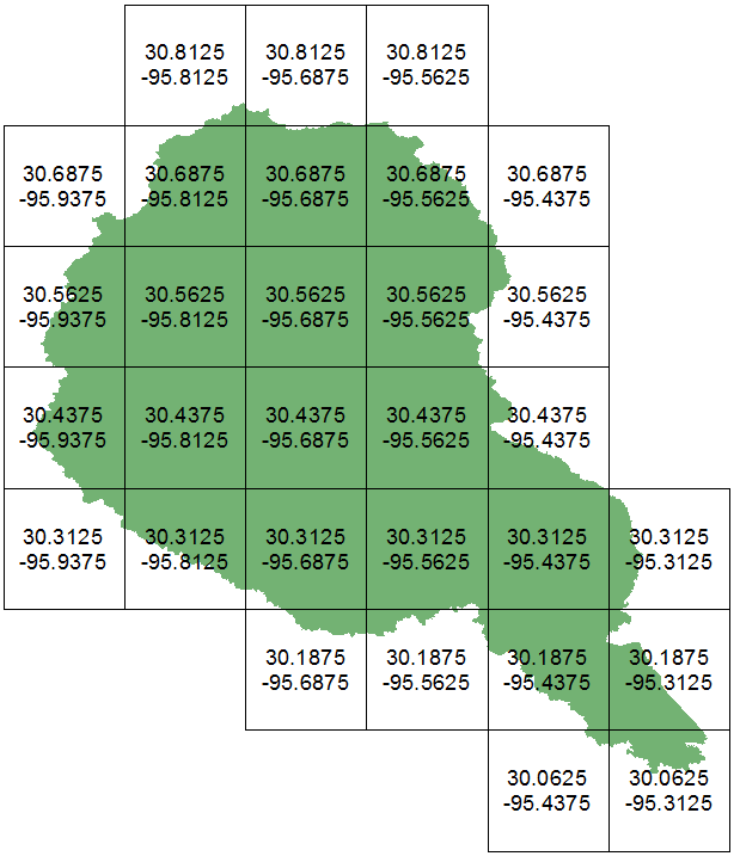

Figure 5. Map of 0.125° grid cells used in model.

2.4.5 VIC Routing Model

The output of the VIC model was implemented with a routing model developed for use with the VIC model (Lohmann et al., 1996; Lohmann et al., 1998). The routing model performs a two-step process of routing the runoff from individual cells to their immediate outlet based on flow direction inputs then performs channel routing based on the Saint-Venant equations (Lohmann et al., 1996; Lohmann et al., 1998).

2.4.6 Model Calibration

Calibration of the VIC model and routing model is most commonly undertaken by adjusting the soil parameters within Table 6. The model was calibrated with streamflow

at USGS stream gauge 08068090 for the period of 2003-2004 then validated to the period of 2005-2010. To assess the calibration and validation the Nash-Sutcliffe coefficient of efficiency (NSE) was used. Calibration and validation results are discussed in Chapter 3.

Table 6. The parameters involved in calibration of the VIC model.

Parameter	Description	Range
Ds	The fraction of Dsmax where non-linear baseflow begins.	>0 to 1
Ds_{max}	The maximum baseflow that can occur within the lowest soil layer (mm/day)	>0 to ~30
Ws	The fraction of maximum soil moisture where non-linear baseflow occurs	>0 to 1
b_{inf}	The amount of available infiltration capacity as a function of relative saturated gridcell area.	>0 to ~0.4

2.5 Climate Change and Land Cover Scenarios

2.5.1 Climate Scenario Data

To simulate the effects of climate change the downscaled CMIP5 projections from the ACCESS1.0 global circulation model (GCM) were obtained for 2070-2090 based on climate scenario Representative Concentration Pathway 8.5 (RCP8.5) which represents a pathway of high greenhouse gas emissions (Ackerley and Dommenget, 2016; Brekke et al., 2013; Van Vuuren et al., 2011). The ACCESS1.0 GCM was chosen as it is one of the more recent GCMs and was designed to reduce biases from land surface temperatures on the atmospheric circulation (Ackerley and Dommenget, 2016). This climate scenario is commonly referred to as the "business as usual" pathway because it assumes human activity continues along the same development path (no significant mitigation). This is why this scenario was chosen, as it may prove to be the likeliest to occur. The downscaled

data were obtained at the 1/8th degree resolution which includes daily precipitation (mm), minimum and maximum daily temperature (°C). Wind values from the Maurer et al. (2002) were reused. This scenario will henceforth be referred to as the RCP8.5 scenario.

2.5.2 Urbanization Scenario Data

To simulate the growth of urban land use, the USGS Earth Resources Observation and Science (EROS) LandCarbon LULC scenario based on the A2 climate scenario from the Special Report on Emissions Scenarios (SRES) was used and will be henceforth mentioned as the LULC-A2 scenario (EROS, 2013). The RCP scenarios are more recent and improve upon the SRES scenarios, but newer EROS scenarios have not yet been performed. However, the A2 scenario family is the closest SRES scenario to the RCP8.5 scenario (Van Vuuren and Carter, 2014). Using the percent increases to developed land within grid cells from the EROS scenarios, the urban land cover was expanded and the vegetation parameters file was modified accordingly.

2.5.3 VIC Model Setup for Future Scenarios

Three future scenarios were simulated: a climate change scenario, a land use change scenario, and a combined scenario. The climate change scenario was based on the RCP8.5 meteorological forcing data. The LULC-A2 scenario was based on present day meteorological forcings and the predicted future land use. Lastly, the combined scenario included both the RCP8.5 meteorological forcing data and the LULC-A2 scenario based urbanization.

2.5.4 Scenario Analysis

To analyze the effects of changes to land use and climate the model outputs were compared to modeled historical baseline period of 2000-2009 from which the model was calibrated and validated. Monthly, seasonal, and annual streamflows were compared between scenarios to quantify and determine which changes to the watershed will be expected to have the greatest effect on future streamflows.

3. RESULTS AND DISCUSSION

3.1 Streamflow Analysis Results

The mean monthly streamflow at USGS stream gauge 08068000 (Figure 6) exhibits a decreasing trend during the period of record from water year 1974 to 2016. This is evidenced by the negative Mann-Kendall tau values for both the Mann-Kendall and Seasonal Mann-Kendall trend tests (Table 7). The calculated Sen's Slope, reported in Table 7, is in accordance with this as well. All three tests indicate that the null hypothesis of no trend can be rejected. The p-values for the Sen's Slope are the same as Mann-Kendall test p-values.

The mean monthly streamflow at USGS stream gauge 08068090 (Figure 7) also exhibits a downward trend over its full period of record from water year 1984 to 2016. The downward trend is considered significant for the Seasonal Mann-Kendall Test with a p-value of 0.04 while the regular Mann-Kendall test fails to reject the null hypothesis of no trend at a 95% confidence level (Table 7). Additionally, neither of the Mann Kendall tests nor the Sen's Slope results were significant for either the first or second period of record for this stream gauge site. Mann Kendall's tau values for the first period of record indicate a possible upward trend while the second period of record's tau values indicate a possible downward trend, but again the null hypothesis for both of these cannot be rejected.

Overall, both stream gauge sites exhibit a significant downward trend in streamflow for their respective periods of record. The gap in record at the downstream site

prevents the Sen's Slope estimation, but the upstream site provided an estimated slope of -0.160 with an upper limit (UL) of -0.058 and a lower limit (LL) of -0.284 (Table 7).

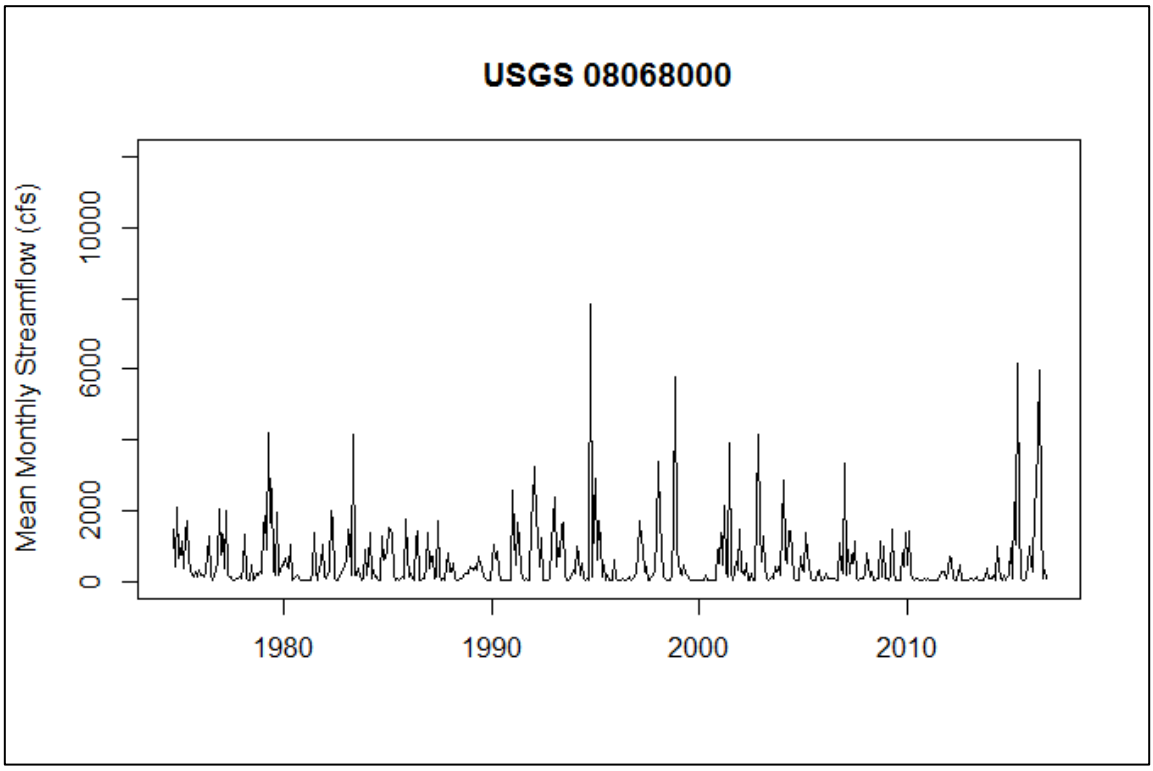

Figure 6. Mean monthly streamflow (cfs) of the WFSJ River near Conroe, USGS 08068000 for the period of 1974 to 2016.

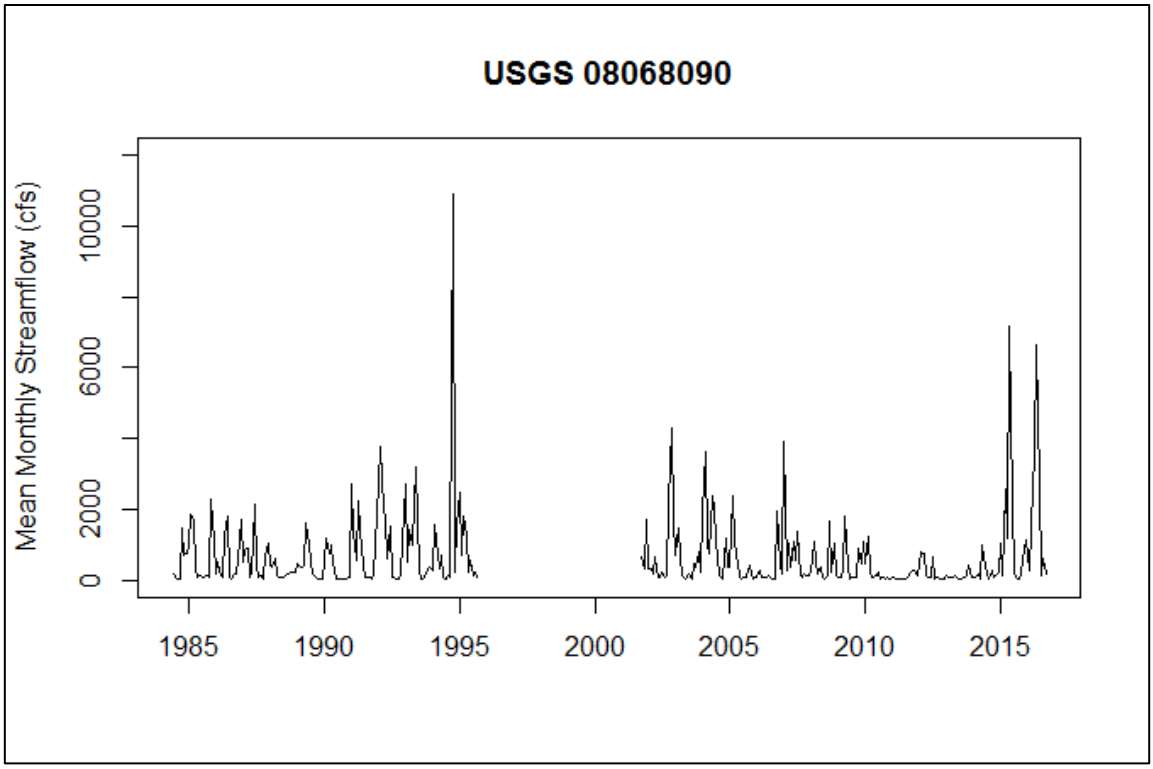

Figure 7. Mean monthly streamflow (cfs) of the WFSJ River above Lake Houston near Porter, USGS 08068090 for the period of 1984 to 2016.

Table 7. Trend analysis results for monthly mean streamflows.

Monthly Streamflow							
Site	Mann-Kendall		Seasonal Mann-Kendall		Sen's slope (95%)		
	Tau	*p-value*	*Tau*	*p-value*	*Slope*	*LL*	*UL*
08068000	-0.102	0.001	-0.110	0.000	-0.160	-0.284	-0.058
08068090 - Full	-0.071	0.060	-0.082	0.040	na	na	na
08068090 - Period 1	0.056	0.337	0.061	0.665	0.273	-0.790	2.032
08068090 - Period 2	-0.072	0.151	-0.086	0.123	-0.332	-0.946	0.120

3.1.1 Seasonal Trend Decomposition

Robust STL decomposition results for the WFSJ River near Conroe, Texas are shown in Figure 8, Figure 9, & Figure 10. The robust STL decomposition with a 3-year trend window shows significant interannual variability, but there is also an overall decrease from 1980 to 2000 (Figure 8). An increasing trend occurs from 2000 to about

2005 during a relatively wet period. A downward trend is again present until about midway through 2013 due to a severe drought that began in 2010. From 2013 until the end of the time-series, there is an increasing trend as a result of high streamflow events in 2015 and 2016. The robust STL with a 5-year trend shows similar results as the 3-year trends, but it is somewhat smoother (Figure 9).

Overall, the analysis of observed streamflow data indicates that from 1980 until 2000 there was a gradual downward trend in streamflow, but streamflow was still relatively stable. The 2000s appear to have been a wet period, but without any abnormally high values. In contrast, the 2010s have been a tale of extremes starting with severe drought turning into abnormally high flow. The extreme drought created enough of an influence that the 7-year trend shows a steep downward trend from 2003 to about the middle of 2012 (Figure 10).

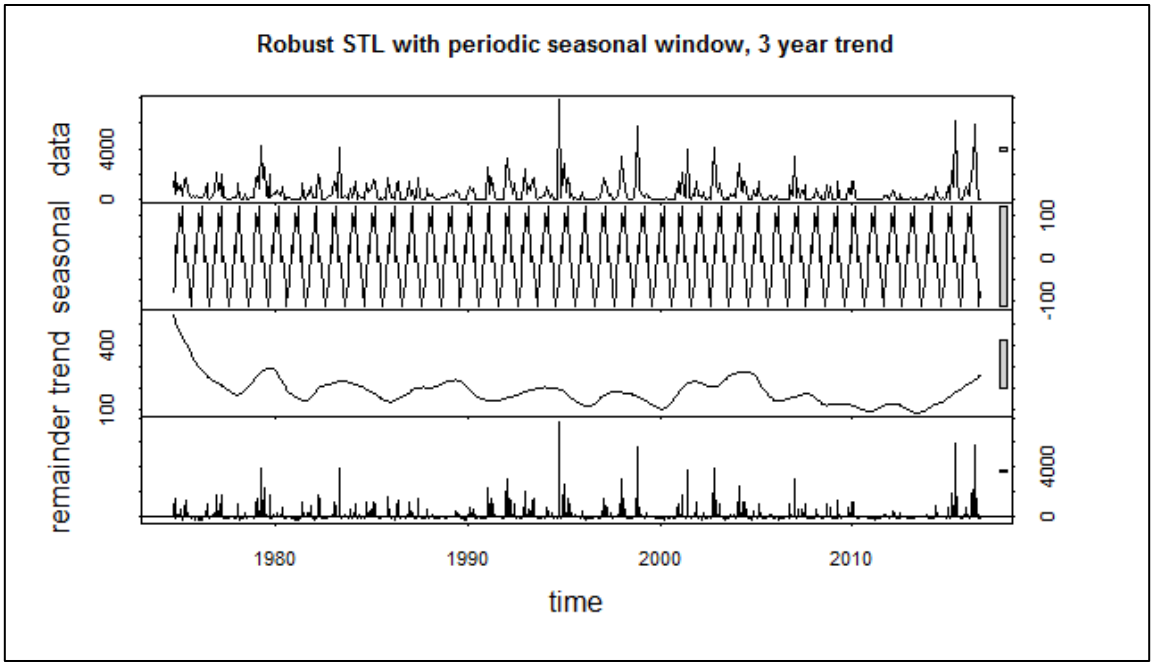

Figure 8. Robust STL decomposition of streamflow at USGS 08068000 with a periodic seasonal window and a 3-year trend window.

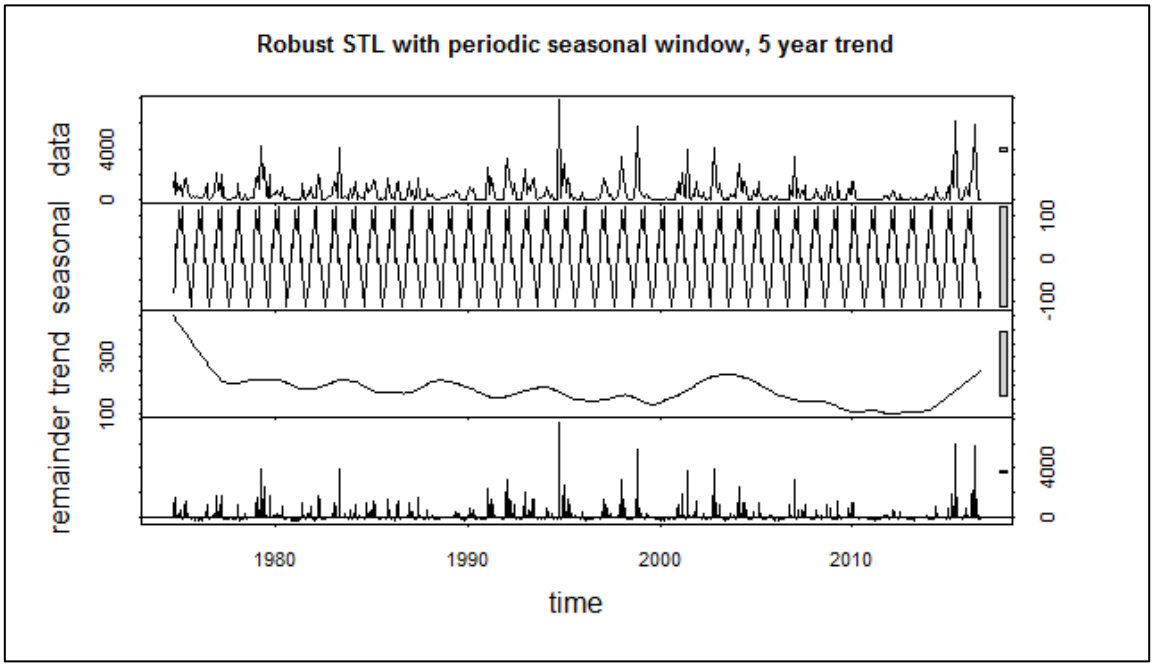

Figure 9. Robust STL decomposition of streamflow at USGS 08068000 with a periodic seasonal window and a 5-year trend window.

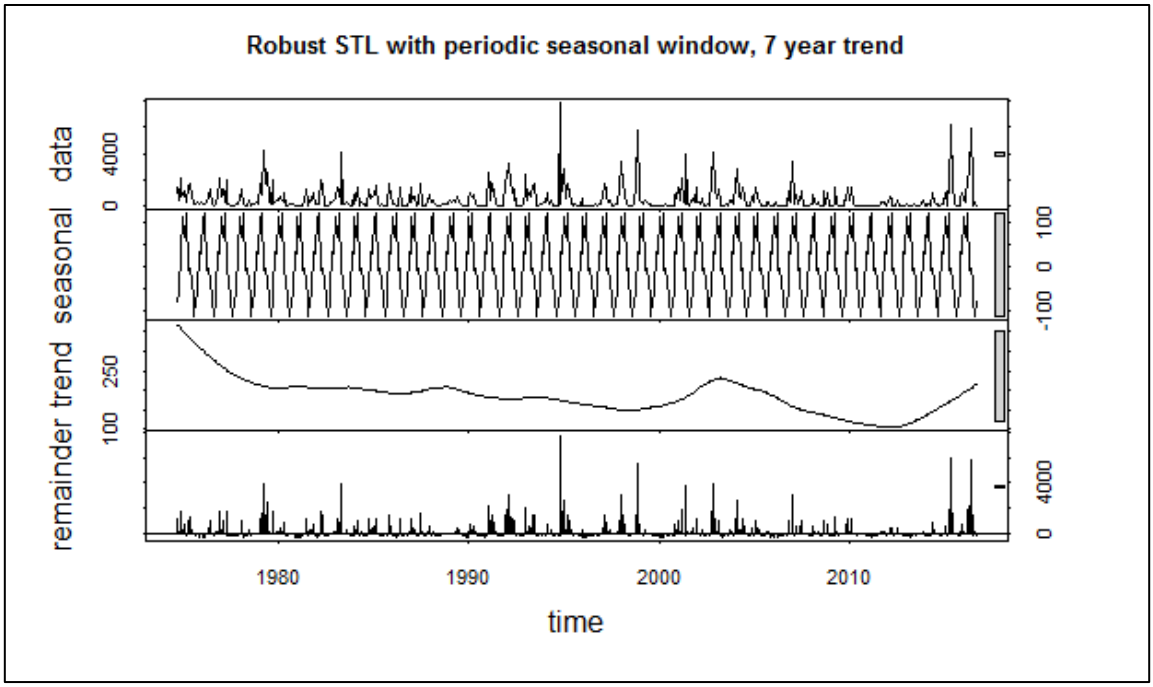

Figure 10. Robust STL decomposition of streamflow at USGS 08068000 with a periodic seasonal window and a 7-year trend window.

3.1.2 Flow Distribution

Results for the streamflow distribution (T_{qmean}) calculations at USGS 08068000 (Figure 11) and USGS 08068090 (Figure 12) indicate potential downward trends due to the Mann-Kendall tau values for their complete period of records, but the trend test failed to reject the null hypothesis for both sites and periods (Table 8).

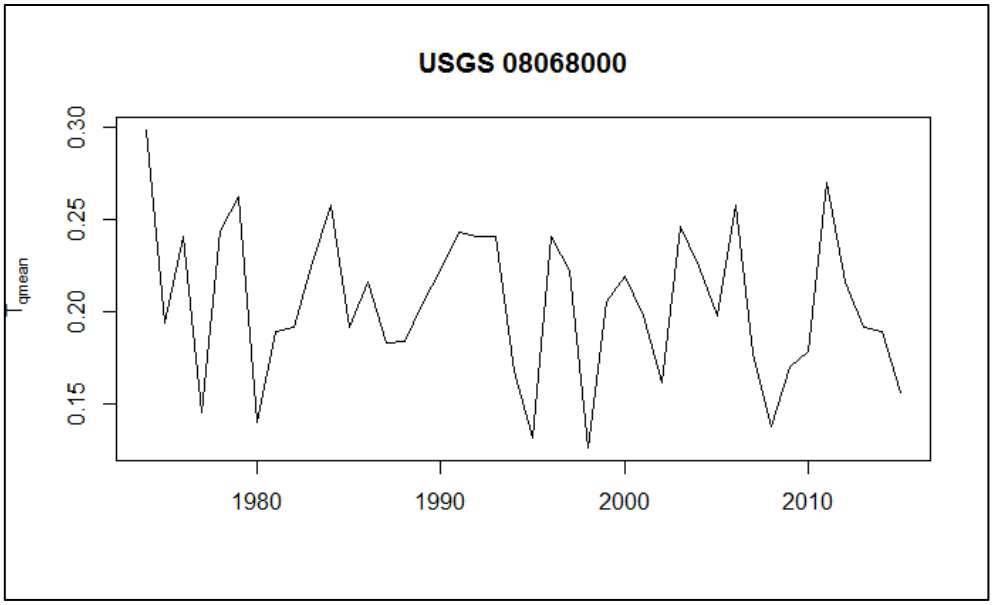

Figure 11. Flow distribution at USGS 08068000.

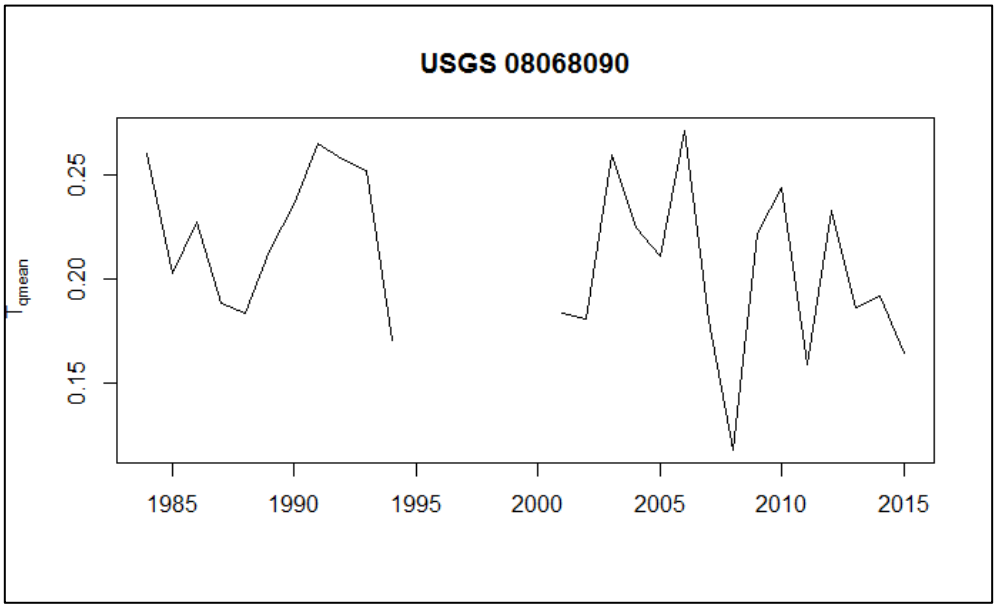

Figure 12. Flow distribution at USGS 08068090.

Table 8. Flow distribution trend analysis results.

T_{qmean}					
Site	Mann-Kendall		Sen's slope (95%)		
	Tau	*p-value*	*Slope*	*LL*	*UL*
08068000	-0.151	0.165	-0.001	-0.002	0.000
08068090 - Full	-0.210	0.140			
08068090 - Period 1	0.018	1.000	0.001	-0.007	0.011
08068090 - Period 2	-0.143	0.488	-0.002	-0.009	0.004

3.1.3 Daily Streamflow Variation

Results of the R-B Index calculations at USGS 08068000 (Figure 13) indicate a possible upward trend of stream flashiness based on the resulting Mann-Kendall tau value, however the resulting p-value is not adequate to reject the null hypothesis of no trend at a 95% confidence level (Table 9). Similarly, the R-B Index results at USGS 08068090 (Figure 14) show a possible upward trend for the full period of record due to the positive Mann-Kendall tau value, but the p-value is also not adequate to reject the null hypothesis of no trend.

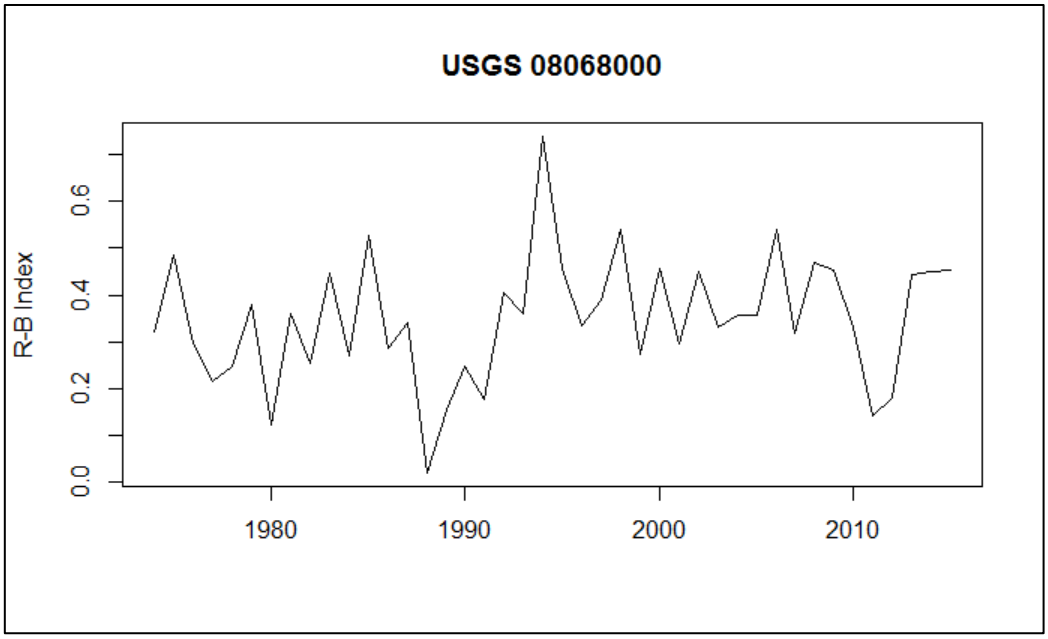

Figure 13. R-B Index of USGS 08068000.

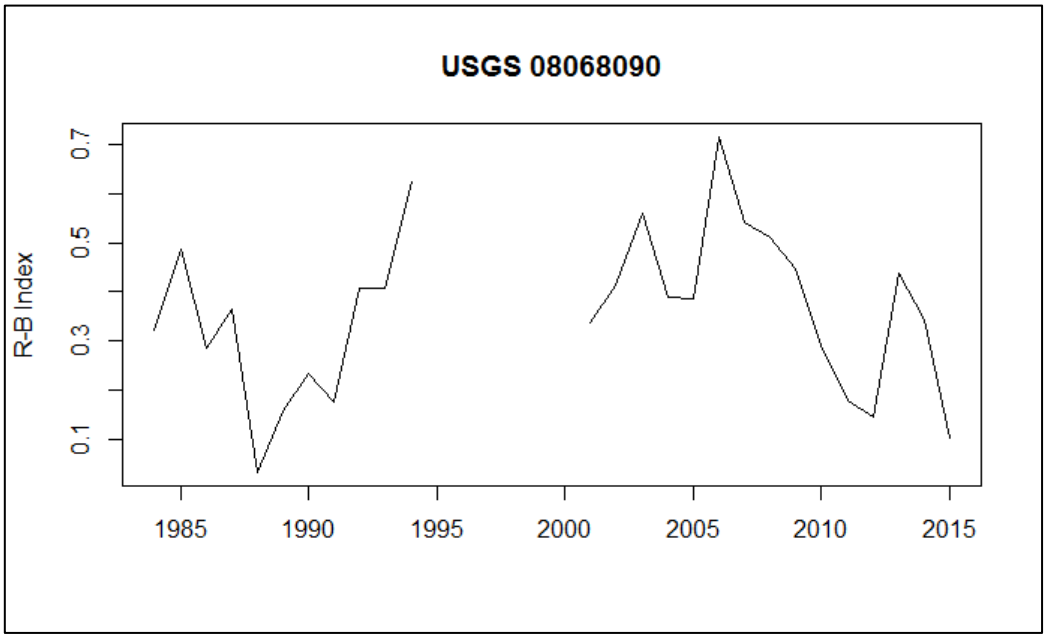

Figure 14. R-B Index of USGS 08068090.

Table 9. R-B Index trend analysis results.

R-B Index					
Site	Mann-Kendall		Sen's slope (95%)		
	Tau	*p-value*	*Slope*	*LL*	*UL*
08068000	0.166	0.124	0.003	0.000	0.006
08068090 - Full	0.040	0.791			
08068090 - Period 1	0.164	0.533	0.011	-0.332	0.079
08068090 - Period 2	-0.371	0.060	-0.019	-0.038	0.000

3.1.4 High Flow Frequency

Results of the High Flow Frequency calculations at USGS 08068000 (Figure 15) and USGS 08068090 (Figure 16) both show a possible downward trend due to their Mann-Kendall tau values, however the trend test failed to reject the null hypothesis of no trend for both sites and periods (Table 10).

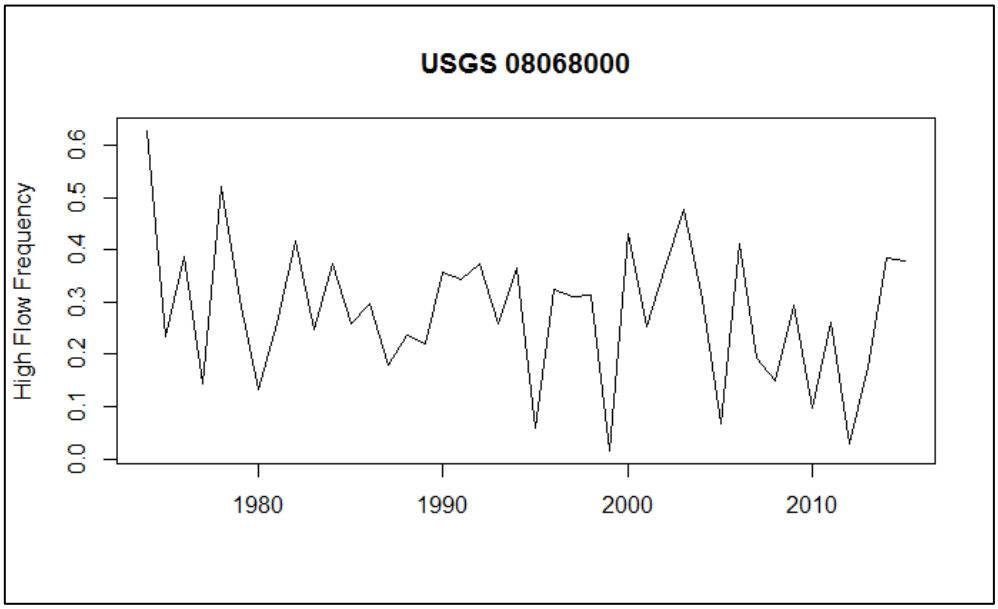

Figure 15. High flow frequency at USGS 08068000.

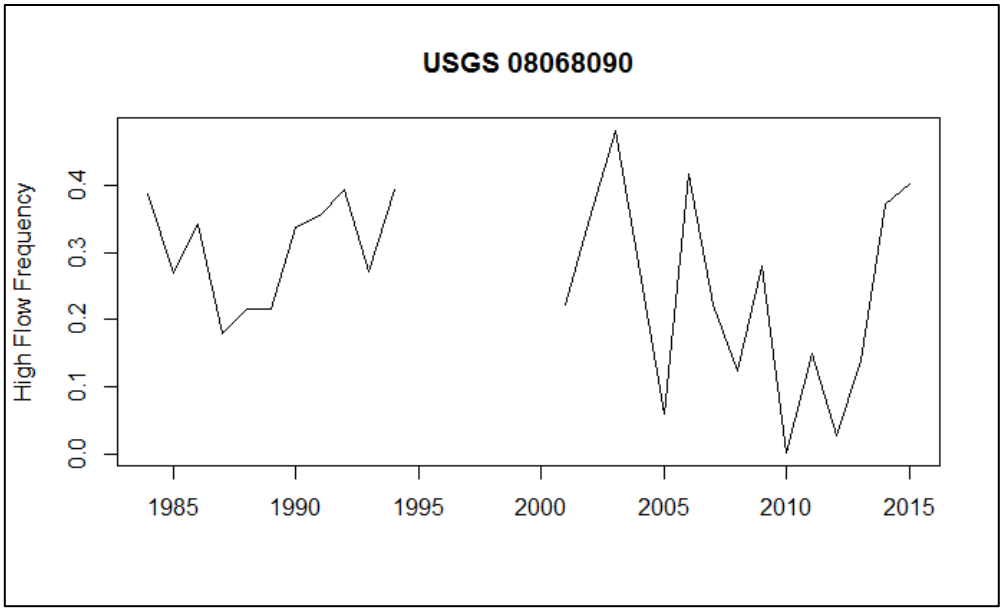

Figure 16. High flow frequency at USGS 08068090.

Table 10. High flow frequency trend analysis results.

High Flow Frequency					
Site	Mann-Kendall		Sen's slope (95%)		
	Tau	*p-value*	*Slope*	*LL*	*UL*
08068000	-0.101	0.351	-0.002	-0.005	0.002
08068090 - Full	-0.111	0.440			
08068090 - Period 1	0.278	0.278	0.011	-0.013	0.031
08068090 - Period 2	-0.124	0.553	-0.007	-0.034	0.016

3.1.4 Land Use/Land Cover Change Results

The results of the NLCD LULC area tabulations and simplification are shown in Table 11. From 2001 to 2006 and 2006 to 2011 the urbanized land cover within the WFSJ watershed increased by 1.43% and 1.15%. This represents an increase in urban land cover of 36.45 km^2 and 29.31 km^2 respectively, for a total gain of 65.76 km^2 from 2001-2011. This represents a gain of 6.58 km^2 in urbanized land cover per year. Additionally, from 2001 to 2011, according to area tabulation of the NLCD PDI, the percent impervious coverage of the watershed increased from 3.10% to 4.01% of the entire watershed.

If the NLCD 1992 dataset is assumed to be as accurate in its representation of the 2001-2011 datasets then we see an increase in total urbanized land cover of 6.77% from 1992 to 2001, making it the more intense rate of growth than the 2000s. However, as previously mentioned, the 1992 data were completed using a different methodology and thus any comparison between 1992 and 2001 must be interpreted with caution.

Table 11. Results of LULC Area Tabulations and Simplification.

Simplified NLCD Class	*NLCD 1992**	NLCD 2001	NLCD 2006	NLCD 2011
Water	*3.75%*	3.81%	3.84%	3.97%
Urbanized	*5.39%*	12.16%	13.59%	14.70%
Forested	*52.60%*	36.20%	34.97%	35.44%
Agricultural	*32.79%*	37.08%	37.15%	35.53%
Wetland	*5.47%*	10.74%	10.44%	10.36%

3.1.5 Discussion

The only significant trend identified during the period of record was a downward trend in mean monthly streamflow at both sites. The shorter period of records, before and after the gap in sampling, at the downstream site did not show a significant trend. This is likely due to the short period of record available for the first and second period of record. The decline in streamflow is matched by the downward trend observed in the STL decomposition results.

Urbanized area within the WFSJ increased from 5.39% in 1992 to 14.70% in 2011 (Table 11). This represents a gain in developed area of roughly 1,226 American football fields per year. In spite of this urban growth, there is a lack of significant trends in flow distribution, daily streamflow variation, and high flow frequency. This may indicate that the streamflow data is inadequate due to the gap of data for USGS 08068090. It is also

possible that urbanization within the watershed has not yet reached a tipping point or that the tipping point is too recent to signify a trend. Yang et al. (2010) found that 3 to 5% impervious surface should be the detectable threshold for the effects of urbanization on a watershed. Additionally, other studies that have successfully detected trends using a variety of indices tend to be conducted on watersheds with more significant amounts of impervious surfaces typically greater than 10% of the watershed (Aulenbach et al., 2017; Diem et al., 2018). Thus, it is a reasonable explanation that the developed imperviousness has not yet reached a tipping point.

Another possibility is that the influence of dam operations at Lake Conroe is great enough that the trends are reduced in their magnitude, making them more difficult to detect. Streamflow records of pre and post-dam conditions are not common, but Schmidt and Wilcock (2008) found that flood event magnitudes were reduced by 60% following dam construction on the Colorado River in the Grand Canyon. Lake Conroe will only release water when the reservoir is full as its primary purpose is water supply, and not flood control. During the events of Hurricane Harvey, for example, the dam reached capacity and released water to prevent damage to the dam and catastrophic failure. The released water was estimated to be about 40% of the flood waters immediately downstream of the dam (Stuckey, 2017).

Reduction in monthly streamflows could signify that this watershed is going to be less reliable in the future as a source of water. It is intuitive that a growing population will need more water. Not only for the purposes of municipal supply but also for industry, recreation, and ecosystem services. Thus, it is important for decision makers to have a

wide range of plans available for the many possible paths the future may take and what they mean for the water resources that they manage.

3.2 VIC Model Results

3.2.1 Calibration and Validation of VIC Model

The VIC model was calibrated to the year of 2003 and validated to the USGS 08068090 data for years of 2003-2004 to reduce computation time because it was being run using the full energy balance mode. The soil parameters that have the most influence over the resulting hydrographs are the infiltration curve shape (b_{inf}), the maximum base flow that can occur from the lowest soil layer (Ds_{max}), the fraction of Ds_{max} where non-linear base flow occurs (Ds), the fraction of the maximum soil moisture where non-linear base flow occurs (Ws), and the thickness of each soil layer (Liang et al., 1994). The calibrated of these parameters are shown in Table 12.

Daily streamflow calibration for 2003 calibration period and the validation period of 2004-2005 returned a NSE value of 0.5003 and 0.31 respectively. Both of these NSE values are considered to be acceptable for daily streamflow (Moriasi et al., 2007). Lake Conroe presents difficulties in modeling the streamflow as releases are not regular and depend upon circumstances that the routing model is not able to represent.

Due to this, the grid cells upstream of Lake Conroe were adjusted to reduce their influence on streamflow. This improved the NSE value to 0.63 and 0.53 for the calibration period (Figure 17) and validation period (Figure 18), respectively. The resulting monthly streamflow values have an NSE value of 0.71 (Figure 19). The non-adjusted routing model outputs better represent the peaks in streamflow while the adjusted routing model better

represents normal, low flow, and monthly streamflows. Due to the primary focus being total streamflows, the adjusted streamflow were utilized for comparisons between future scenarios of land cover and climate change.

Table 12. Table of calibrated VIC parameters.

Parameter	Units	Range	Calibrated Value
b_{inf}	None	0 ~ 0.4	0.03
Ds	None	0 ~ 1	0.015
Ds_{max}	mm/day	0 ~ 30	10
Ws	None	0 ~ 1	0.99
Soil Depth - Layer 1	meters	0.1 ~ 1.5	0.1
Soil Depth - Layer 2	meters	0.1 ~ 1.5	0.9
Soil Depth - Layer 3	meters	0.1 ~ 1.5	0.5

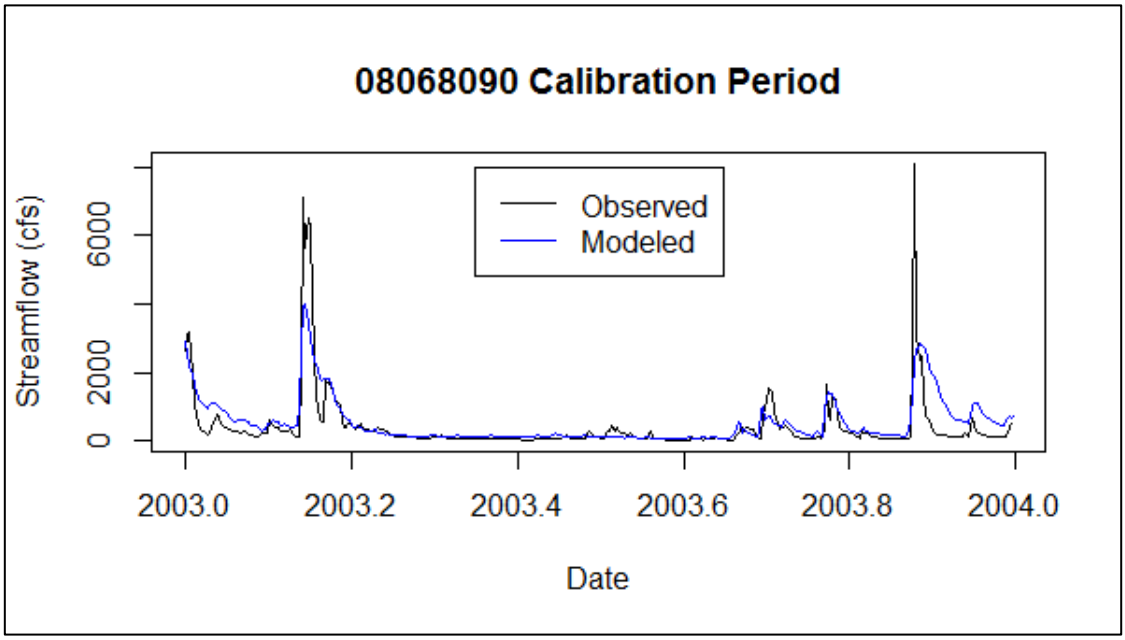

Figure 17. Calibration period results for the VIC model routed to daily streamflow (cfs), from January 1, 2003 to December 31, 2003. NSE = 0.63.

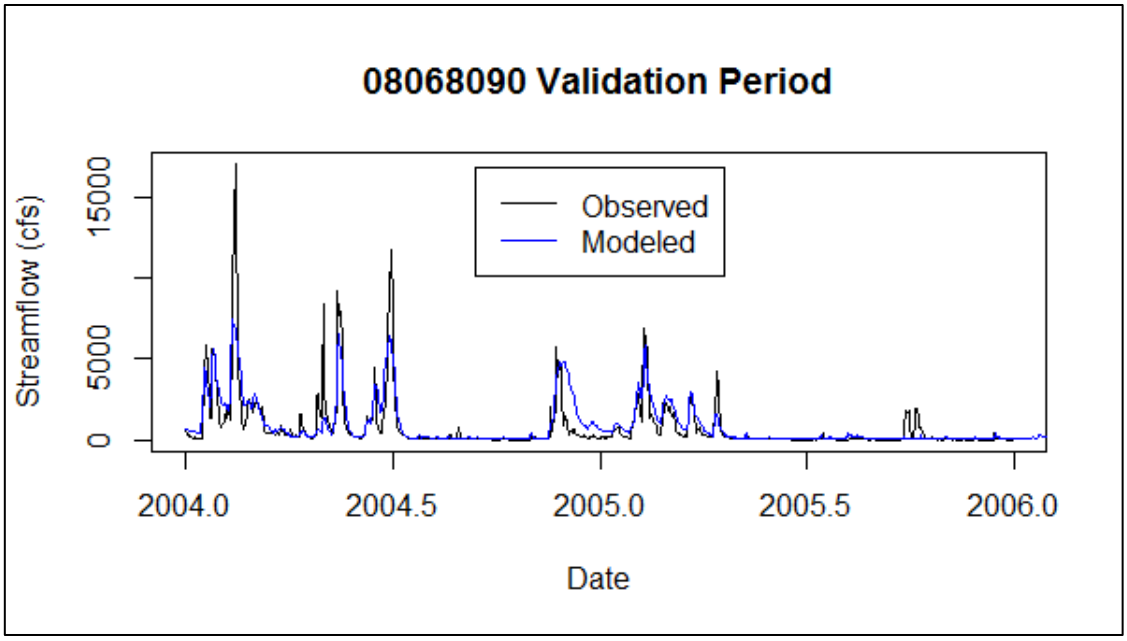

Figure 18. Validation period results of the VIC model routed to daily streamflow (cfs) from January 1, 2004 to December 31, 2005. NSE = 0.53.

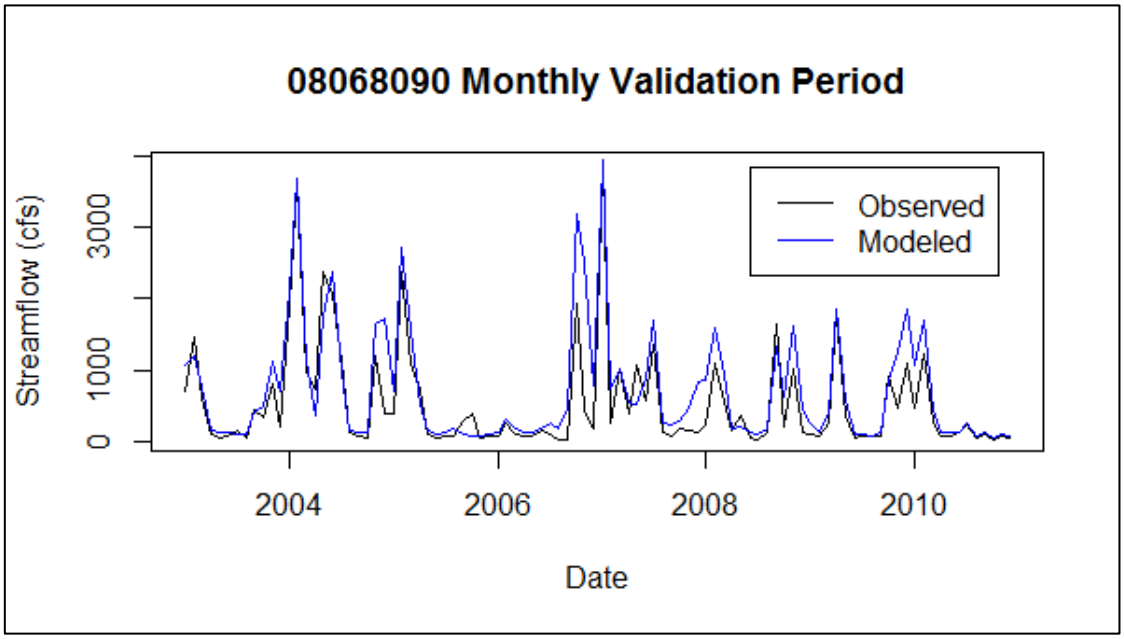

Figure 19. Validation of modeled monthly mean streamflow (cfs) for the period of January 2003 to December 2010. NSE = 0.71.

3.2.2 Results of Land Cover Change Scenario

According to the USGS EROS LandCarbon projections of LULC under SRES climate scenario A2 there is expected to be heavy urbanization occurring in the southeastern regions of the WFSJ watershed and along the northeastern edge as Houston and its suburbs continue to expand. Analysis of the LandCarbon projection in ArcGIS it was estimated that developed land cover within the entire WFSJ watershed will increase by 511% from 2010 coverages by 2090 (Figure 20). The growth within each individual grid cell was calculated and applied to the vegetation parameters file.

As shown in Table 13, developed land increases from about 4% to nearly 20% of the entire watershed area. The greatest changes to land cover occur in the southeastern region of the watershed. This is the location of the greatest amount of urbanization. Another condensed area of developed land emerges at the northeastern corner of the watershed. Woodland and forests exhibit the greatest amount of lost watershed area (Table 13).

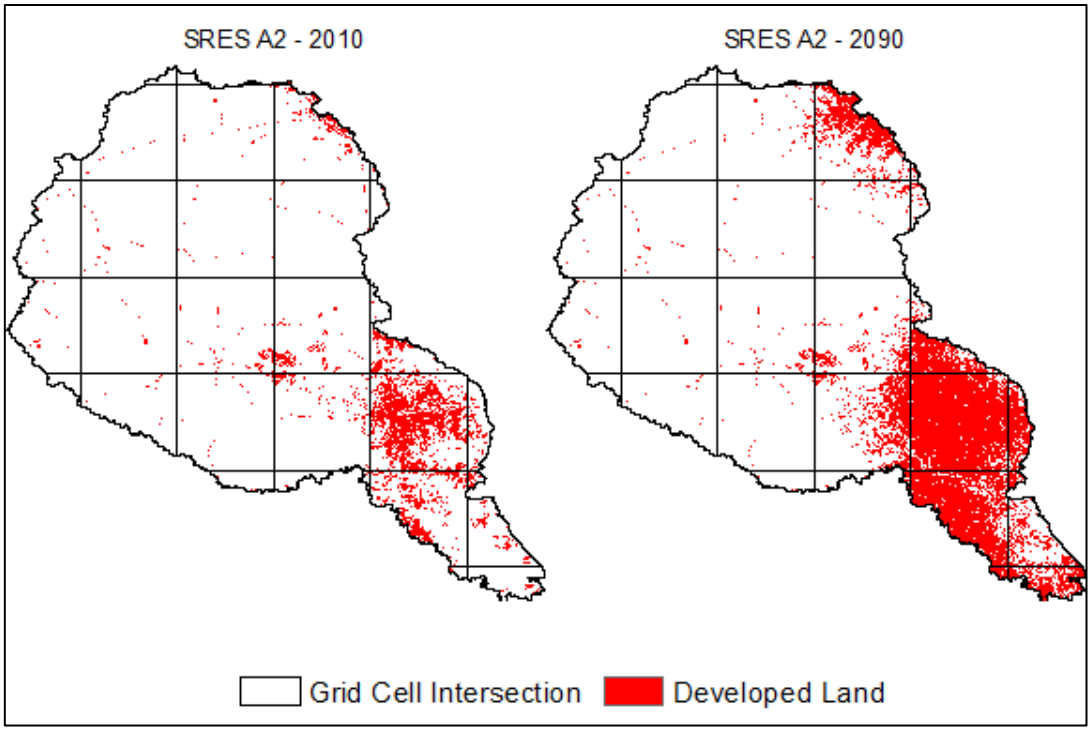

Figure 20. Projected developed land increase in the West Fork San Jacinto watershed according to SRES climate scenario A2.

Table 13. Changes in land use within the WFSJ watershed using urbanization rate from LandCarbon A2 scenario.

Land Cover Class	Baseline		SRES A2	
	Area (km^2)	%	Area (km^2)	%
Forested	219.47	22.32%	192.05	19.53%
Woodland	564.16	57.38%	441.88	44.95%
Grassland/Shrubland	57.93	5.89%	55.26	5.62%
Crops	101.63	10.34%	99.27	10.10%
Developed	39.97	4.07%	194.70	19.80%

The mean monthly streamflow for the 2001-2010 period generally decreased in winter and autumn months and increased in spring and summer months under the LandCarbon A2 scenario (Table 14 & Figure 22). The greatest increases in streamflow occurred in May, July, and September. In grid cell 19725, the developed land cover increased from 24.8% to 93.7% of the area which had the effect of decreasing the VIC

modeled evaporation while increasing the modeled runoff and baseflow (Table 15 &Table 16). Runoff increased for all seasons with the greatest increases occurring during fall and summer, yet streamflow did not. Evaporation had an overall decrease, but had increases in winter and fall while spring and summer had decreases in evaporation.

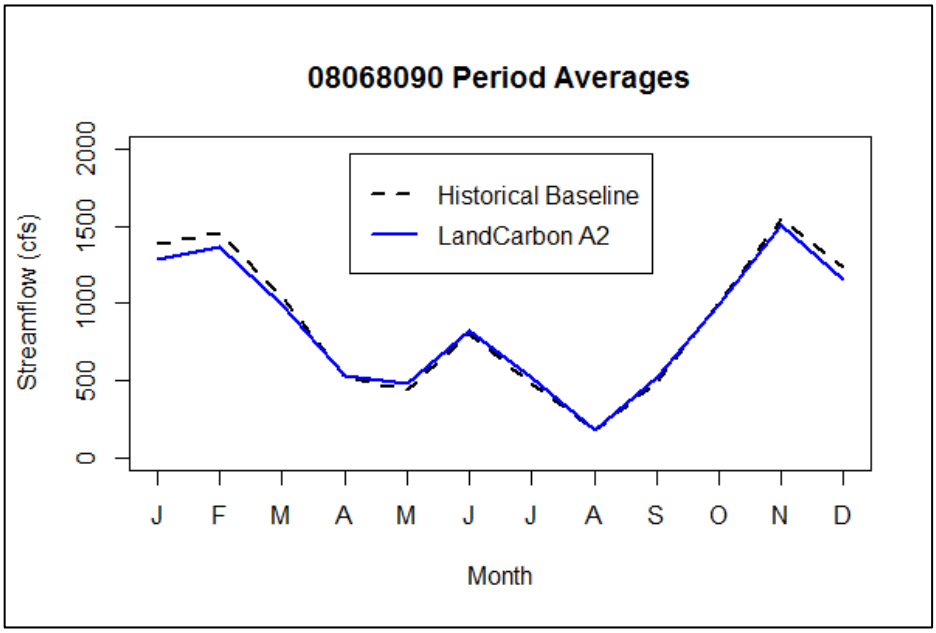

Figure 21. Mean streamflow by month for the Historical Baseline and the LandCarbon A2 scenario.

Table 14. Changes in streamflow from the historical baseline to the LandCarbon A2 landcover change scenario.

Month	Historical Baseline	LandCarbon A2	
	Mean Streamflow (cfs)	Mean Streamflow (cfs)	% Change
Jan	1382.21	1281.72	-7.27%
Feb	1459.62	1362.68	-6.64%
Mar	1040.61	993.31	-4.55%
Apr	523.68	534.09	1.99%
May	436.26	480.89	10.23%
Jun	798.10	822.25	3.03%
Jul	482.45	523.22	8.45%
Aug	176.11	179.00	1.64%
Sep	489.49	518.28	5.88%
Oct	1002.13	996.78	-0.53%
Nov	1552.91	1510.08	-2.76%
Dec	1238.70	1160.14	-6.34%
Annual	881.86	863.54	-2.08%

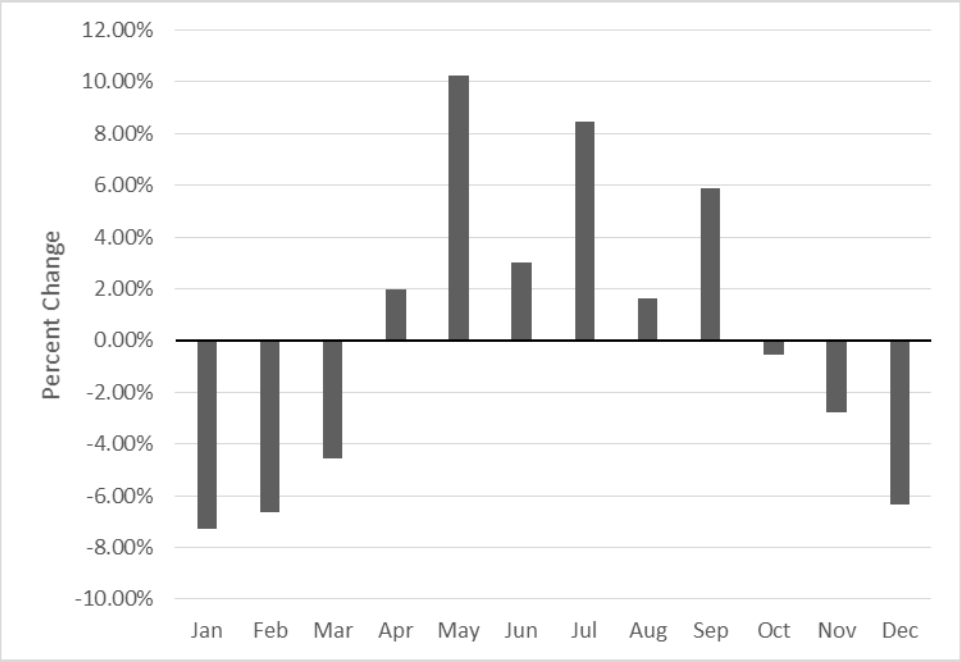

Figure 22. Percent change in monthly modeled streamflow from the historical baseline scenario to the LULC-A2 scenario.

Table 15. Evaporation, runoff, and baseflow, as a fraction of precipitation, within grid cell 19725 from the baseline scenario to the LandCarbon A2 scenario.

	Baseline Scenario			Landcarbon A2 Scenario		
Season	Evaporation	Runoff	Baseflow	Evaporation	Runoff	Baseflow
Winter	0.280	0.024	0.604	0.305	0.026	0.665
Spring	0.805	0.020	0.343	0.639	0.024	0.472
Summer	0.826	0.017	0.175	0.756	0.021	0.263
Fall	0.323	0.037	0.337	0.390	0.061	0.421
Full Period	0.543	0.025	0.352	0.519	0.036	0.441

Table 16. Percent changes to evaporation, runoff, and baseflow, as a fraction of precipitation, within grid cell 19725 from the baseline scenario to the LandCarbon A2 scenario.

Season	Evaporation	Runoff	Baseflow
Winter	8.82%	10.23%	10.13%
Spring	-20.57%	15.30%	37.61%
Summer	-8.50%	26.67%	50.93%
Fall	20.69%	64.87%	24.98%
Full Period	-4.46%	39.60%	25.39%

3.2.3 Results of Climate Change Scenario

Under climate scenario RCP8.5 for the simulated period of 2080-2089 the modeled streamflow decreased in all months (Figure 23 & Table 17). Average annual streamflow decreased by 50.17%. Within the WFSJ watershed, under the RCP8.5 climate scenario, mean daily precipitation is expected to decrease by about 24% with mean daily maximum and minimum temperature increasing by 19% and 22% respectively. Spring and summer see the greatest decreases in streamflow, with the greatest monthly decreases being in March, June, and July. Although mean daily precipitation is expected to decrease, the total precipitation for the period of record increased by 2.64% in the RCP8.5 scenario.

Within grid cell 19725, the greatest change between the baseline scenario the RCP8.5 scenario is that of evaporation. Evaporation, as a percentage of precipitation, increased by nearly doubled (Table 21). Additionally, under scenario RCP8.5 show that the number of days with precipitation increases, but most of these days will only have trace to small amounts of precipitation (Table 22 Table 23).

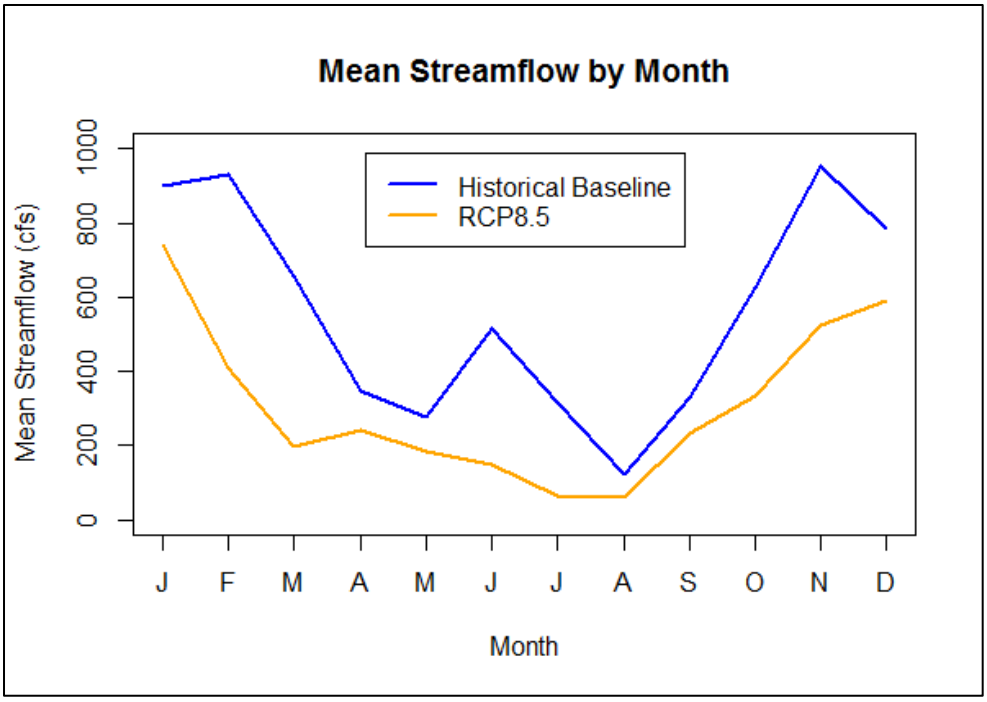

Figure 23. Mean streamflow by month for the Historical Baseline and the RCP8.5 scenario.

Table 17. Changes in streamflow from the historical baseline to the RCP8.5 climate change scenario.

Historical Baseline	RCP8.5	
Mean Streamflow (cfs)	Mean Streamflow (cfs)	% Change
1382.21	1056.63	-23.56%
1459.62	575.92	-60.54%
1040.61	267.52	-74.29%
523.68	343.23	-34.46%
436.26	253.60	-41.87%
798.10	200.36	-74.90%
482.45	76.06	-84.23%
176.11	72.30	-58.94%
489.49	323.19	-33.98%
1002.13	471.77	-52.92%
1552.91	774.66	-50.12%
1238.70	858.10	-30.73%
881.86	439.44	-50.17%

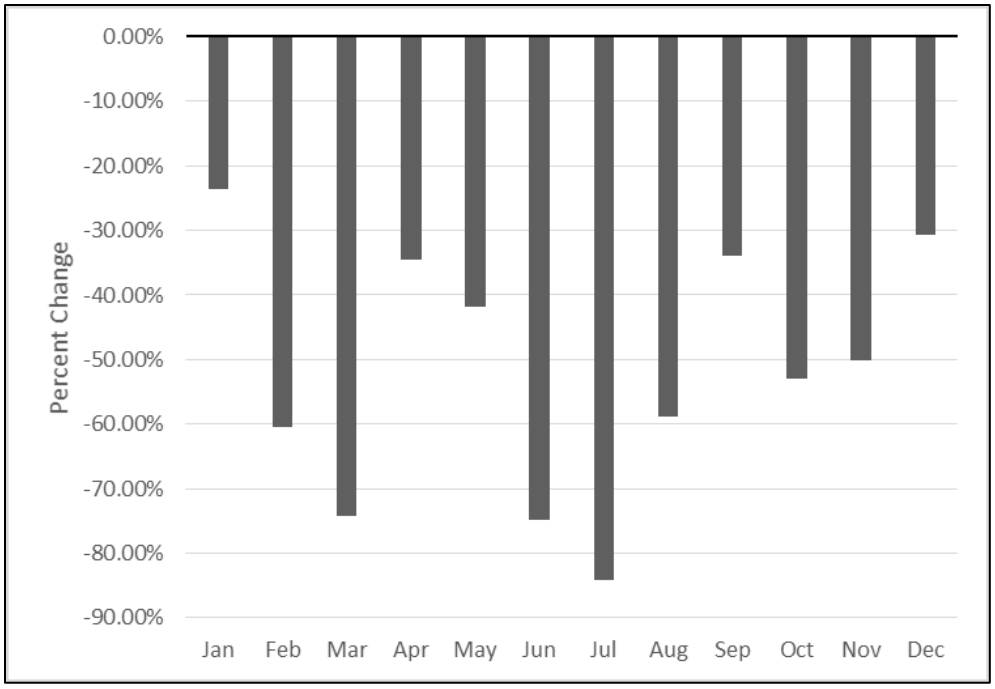

Figure 24. Percent change in modeled monthly streamflow from 2001-2010 to the RCP8.5 climate change scenario of 2080-2089.

Table 18. Comparison of seasonal streamflow between the historical baseline and RCP8.5 scenarios.

Season	Historical Baseline	RCP8.5	
	Mean Streamflow (cfs)	Mean Streamflow (cfs)	% Change
Winter	1360.18	830.22	-38.96%
Spring	666.85	288.11	-56.79%
Summer	485.55	116.24	-76.06%
Fall	1014.85	523.21	-48.44%

Table 19. Total precipitation by month for the Historical Baseline scenario and the RCP8.5 scenario.

Month	Baseline Precipitation (mm)	RCP8.5 Precipitation (mm)	Percent Change (%)
Jan	935.34	937.75	0.26%
Feb	925.99	462.29	-50.08%
Mar	912.38	567.3	-37.82%
Apr	660.99	906.67	37.17%
May	933.44	1138.74	21.99%
Jun	1441.51	458	-68.23%
Jul	1015.06	299.88	-70.46%
Aug	964.16	470.43	-51.21%
Sep	979.27	955.77	-2.40%
Oct	1799.79	1093.75	-39.23%
Nov	1367.6	1560.8	14.13%
Dec	868.76	835.2	-3.86%
Full Period	12804.29	9686.58	-24.35%

Table 20. Evaporation, runoff, and baseflow, as a fraction of precipitation, within grid cell 19725 from the baseline scenario to the RCP8.5 scenario.

Season	Baseline			RCP8.5		
	Evaporation	Runoff	Baseflow	Evaporation	Runoff	Baseflow
Winter	0.280	0.024	0.604	0.407	0.022	0.417
Spring	0.805	0.020	0.343	0.812	0.015	0.135
Summer	0.826	0.017	0.175	1.696	0.006	0.077
Fall	0.323	0.037	0.337	0.348	0.016	0.117
Full Period	0.54	0.03	0.35	0.66	0.02	0.19

Table 21. Percent change in precipitation and evaporation, runoff, and baseflow, as fractions of precipitation, within grid cell 19725 from the baseline scenario to the RCP8.5 scenario.

Season	Precipitation (% change)	Fraction of Precipitation (% change)		
		Evaporation	Runoff	Baseflow
Winter	-18.13%	45.39%	-7.79%	-31.04%
Spring	4.22%	0.94%	-25.88%	-60.61%
Summer	-64.09%	105.28%	-61.43%	-55.68%
Fall	-12.93%	7.58%	-56.04%	-65.19%
Full Period	-24.35%	21.20%	-37.29%	-47.09%

Table 22. Percent change, from the baseline scenario to the RCP8.5 scenario, in the number of days with precipitation, moderate rainfall, and heavy rainfall.

Season	Precipitation Days (% of All Days)	Percent of Precipitation Days with Moderate Rain (2.54 to 7.62 mm)	Percent of Precipitation Days with Heavy Rain (> 7.62 mm)
Winter	34.53%	2.01%	-44.46%
Spring	77.00%	14.43%	-35.57%
Summer	45.50%	-25.32%	-80.75%
Fall	50.82%	75.67%	-18.66%
Annual	51.05%	11.32%	-46.85%

Table 23. Breakdown of the number of days for the Baseline and RCP8.5 scenarios.

	Number of Days with Precipitation					
Scenario	Trace	< 25 mm	< 50 mm	< 75 mm	< 100 mm	>100 mm
Base	1188	239	101	26	11	7
RCP8.5	1795	402	55	9	5	1

3.2.4 Results of Combined Climate and Land Cover Change Scenario

Under the combined RCP8.5 and LULC-A2 scenario, the monthly streamflows decreased in for all months compared to the baseline scenario (Table 24). As in the RCP8.5 only scenario, the greatest impacted season was again summer with a reduction of streamflow by 69.8% compared to the historical baseline. Average annual streamflow exhibited a 44.24% decrease from the historical baseline scenario. For grid cell 19725 (Table 26, Table 27, & Table 28), it was found that runoff increases in winter and spring, but is greatly reduced in summer and fall. Baseflow decreases in all months and resulted in a 20.18% reduction for the period. Evaporation only decreased in the spring months and had a 27.3% increase for the period. The greatest increase in evaporation occurred during

summer where it increased 116.76%. Streamflow in all months increased in comparison with the RCP8.5 only scenario.

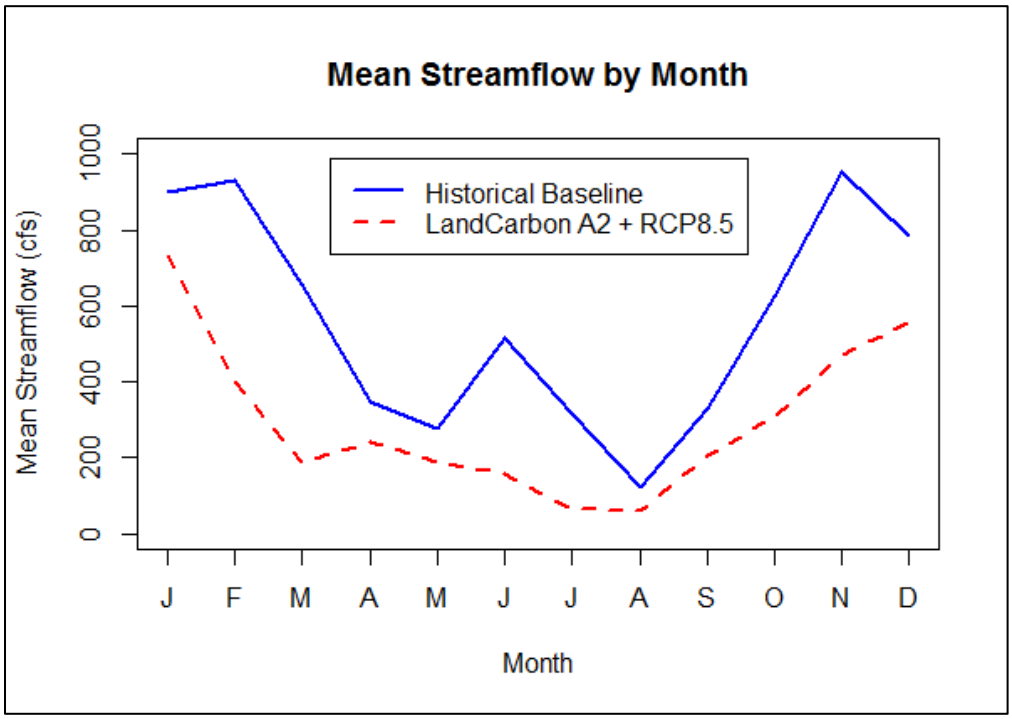

Figure 25. Mean streamflow by month for the Historical Baseline and the combined LandCarbon A2 and RCP8.5 scenario.

Table 24. Changes in streamflow from the historical baseline to the combined RCP8.5 and LULC-A2 scenario.

Month	Historical Baseline	A2 and RCP8.5	
	Mean Streamflow (cfs)	Mean Streamflow (cfs)	% Change
Jan	1382.21	1109.54	-19.73%
Feb	1459.62	619.80	-57.54%
Mar	1040.61	314.86	-69.74%
Apr	523.68	439.58	-16.06%
May	436.26	359.70	-17.55%
Jun	798.10	280.25	-64.88%
Jul	482.45	91.58	-81.02%
Aug	176.11	81.17	-53.91%
Sep	489.49	362.99	-25.84%
Oct	1002.13	490.92	-51.01%
Nov	1552.91	817.09	-47.38%
Dec	1238.70	933.26	-24.66%
Annual	881.86	491.73	-44.24%

Table 25. Changes in seasonal streamflow from the historical baseline to the combined LULC-A2 scenarios.

Season	Historical Baseline	A2 and RCP8.5	
	Mean Streamflow (cfs)	Mean Streamflow (cfs)	% Change
Winter	1360.18	887.53	-34.75%
Spring	666.85	371.38	-44.31%
Summer	485.55	151.00	-68.90%
Fall	1014.85	557.00	-45.12%

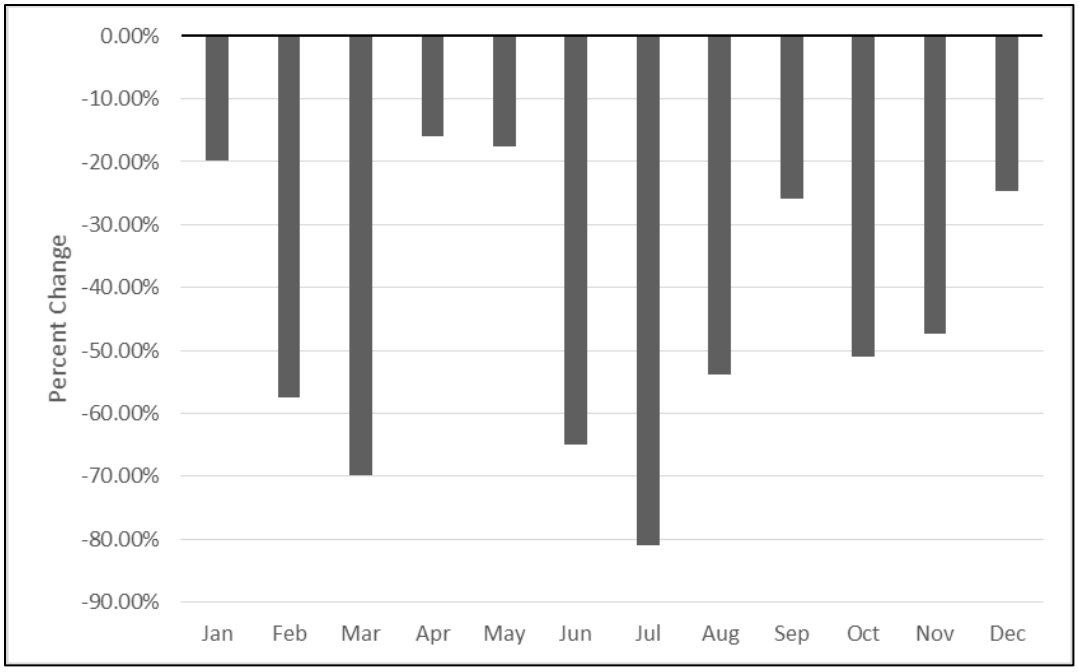

Figure 26. Percent change in modeled monthly streamflow from the historical baseline to the combined RCP8.5 and LULC-A2 scenario.

Table 26. Evaporation, runoff, and baseflow, as a fraction of precipitation, within grid cell 19725 from the baseline scenario to the combined LandCarbon A2 + RCP8.5 scenario.

Season	Baseline			RCP8.5		
	Evaporation	Runoff	Baseflow	Evaporation	Runoff	Baseflow
Winter	0.280	0.024	0.604	0.397	0.025	0.558
Spring	0.805	0.020	0.343	0.664	0.021	0.292
Summer	0.826	0.017	0.175	1.791	0.013	0.162
Fall	0.323	0.037	0.337	0.518	0.019	0.142
Full Period	0.54	0.03	0.35	0.69	0.02	0.28

Table 27. Percent change in precipitation and evaporation, runoff, and baseflow, as fractions of precipitation, within grid cell 19725 from the baseline scenario to the RCP8.5 scenario.

Season	Precipitation (% change)	Fraction of Precipitation (% change)		
		Evaporation	Runoff	Baseflow
Winter	-18.13%	41.69%	5.23%	-7.71%
Spring	4.22%	-17.52%	2.75%	-14.84%
Summer	-64.09%	116.76%	-24.19%	-7.43%
Fall	-12.93%	60.26%	-49.72%	-57.96%
Full Period	-24.35%	27.30%	-21.80%	-20.18%

Table 28. Difference of precipitation fractions from the RCP8.5 only scenario to the combined LandCarbon and RCP8.5 scenario.

Season	Difference from RCP8.5 Scenario		
	Evaporation	Runoff	Baseflow
Winter	-3.70%	13.02%	23.34%
Spring	-18.46%	28.63%	45.77%
Summer	11.48%	37.24%	48.24%
Fall	52.67%	6.32%	7.23%
Full Period	6.09%	15.49%	26.90%

3.2.5 Discussion

The main purpose of this study was to quantify future changes to streamflow annually and seasonally within the WSFJ watershed. Usage of the VIC hydrological model adequately represented the hydrology of the WSFJ watershed and enabled the construction of scenarios that depict future changes to LULC and climate. The historical baseline scenario represented the timeframe of 2001-2010 both in terms of LULC and climate while the LULC-A2 scenario depicted a change in LULC for 2090 with the climate from 2001-2010. Future climate was depicted through the RCP8.5 climate scenario. Additionally, the combined RCP8.5 climate and LULC-A2 scenario combined the two

scenarios of future conditions. Between the three scenarios, the greatest negative effect on seasonal streamflow was exhibited by the RCP8.5 climate change scenario (Table 29).

The changes to developed land through the LandCarbon A2 scenario increased the fraction of runoff and baseflow for both the historical baseline simulation as well as the climate change scenario simulation. This is to be expected with larger amounts of urbanization as the impervious surfaces will convey precipitation to the watercourses faster. From the climate change only scenario to the combine climate and LULC change scenario, evaporation increased for summer and fall, but decreased for winter and spring. Fall, in particular, under the combined scenario had a nearly 53% more of a difference with the baseline in the combined scenario compared to RCP8.5 scenario. Summer, for comparison, only had an 11% difference between the fractions of evaporation. This is possibly due to the summer months receiving much less rainfall, thus there is less evaporation that could be possible. The summer months receive 64% less rainfall under the RCP8.5 climate scenario while fall only receives about 13% less rainfall.

Potential evaporation has been shown to increase with urbanization (Balling and Brazel, 1987). However, actual evaporation has been shown to decrease with urbanization due to the reduced residence time of water in an urbanized setting (Dow and DeWalle, 2000). The two scenarios with the LandCarbon A2 scenario showed differing results, however. The LULC change with the baseline meteorological forcings resulted in a 4.46% reduction in evaporation for the period, while the RCP8.5 climate had a 5.03% increase in evaporation. This could possibly be due to the higher temperatures of the RCP8.5 scenario in conjunction with how impervious cover is represented in VIC as bare soil which has a

lower albedo than vegetation. Thus, water may still infiltrate and moisten the soil as opposed to all of the incoming precipitation becoming runoff.

The season that is most impacted by climate change is the summer months of June, July, August (Table 30). The combined RCP8.5 and LULC-A2 change scenario exhibited a slightly less negative impact on summer, fall, and winter flows. This is likely due to the increased imperviousness that reduces the time water is present. This becomes more evident when comparing the scenarios without the LandCarbon A2 LULC changes to the scenarios with them as runoff increased for all seasons in both scenarios with the LULC changes. Reductions in forested and woodland areas increases the potential for runoff events and increases evaporative losses from soil due to the loss of canopy that would otherwise intercept precipitation and reduce the incoming radiation that reaches the soil (Greenwood, 1992).

While all seasons exhibit a decrease in streamflow under both climate change scenarios, the large decreases in streamflow during spring and summer may further be exacerbated due to higher water demands during this time of year. Lawns and crops require more irrigation during summer while recreation uses rises as people attempt to "beat the heat." Reduced rainfall in these months according to RCP8.5 will mean a greater need for irrigation to grow crops, maintain pasture, and ultimately provide food for a growing population.

Overall the greatest influence was observed from climate change, although changes in land cover have shown the ability to offset, to a small degree, the effects of climate change. This is similar to results found by Liu et al. (2011) who drew similar

conclusions for their watershed. Despite the watershed's primary land conversions were not similar, as the watershed from that study was primarily concerned with agricultural changes, they drew the same conclusions about climate having the greatest effect. Castillo et al. (2014) additionally found the effects of climate change to be the greatest influence upon a coastal Texas watershed where LULC changes again had the ability to influence, negative and positively, future flows.

The results of this study are contrary to a study that modeled regional watersheds in the United States from 2010-2050 and found a 22% increase in annual flow (Naz et al., 2018). However, the Naz et al. (2018) study modeled a different study period and used 4 watersheds across the entire Texas Gulf region, none of which are the WFSJ watershed. This indicates that other watersheds may have increased streamflow in the future and it will be worth conducting other studies within the Texas Gulf region to provide better resolution moving forwards.

Another factor to consider is that this LULC change features large amounts of urbanization, which implies population growth which will further increase water demand and stress water resources. Thus the negative impacts shown in the LULC-A2 scenarios may be worse as future extractions of the river rise to meet water demands. Hoekema et al. (2010) found that irrigation shortages by 2050 in the Payette River in Idaho will see irrigation shortages of 9% which they postulate will be exacerbated by expanding cities and growing populations. This is similar to the problems facing the WFSJ watershed. The reality of the situation is that while water is a renewable resource, it is still a limited

resource and the need for sustainable management will continue to grow as temperatures and populations continue to rise.

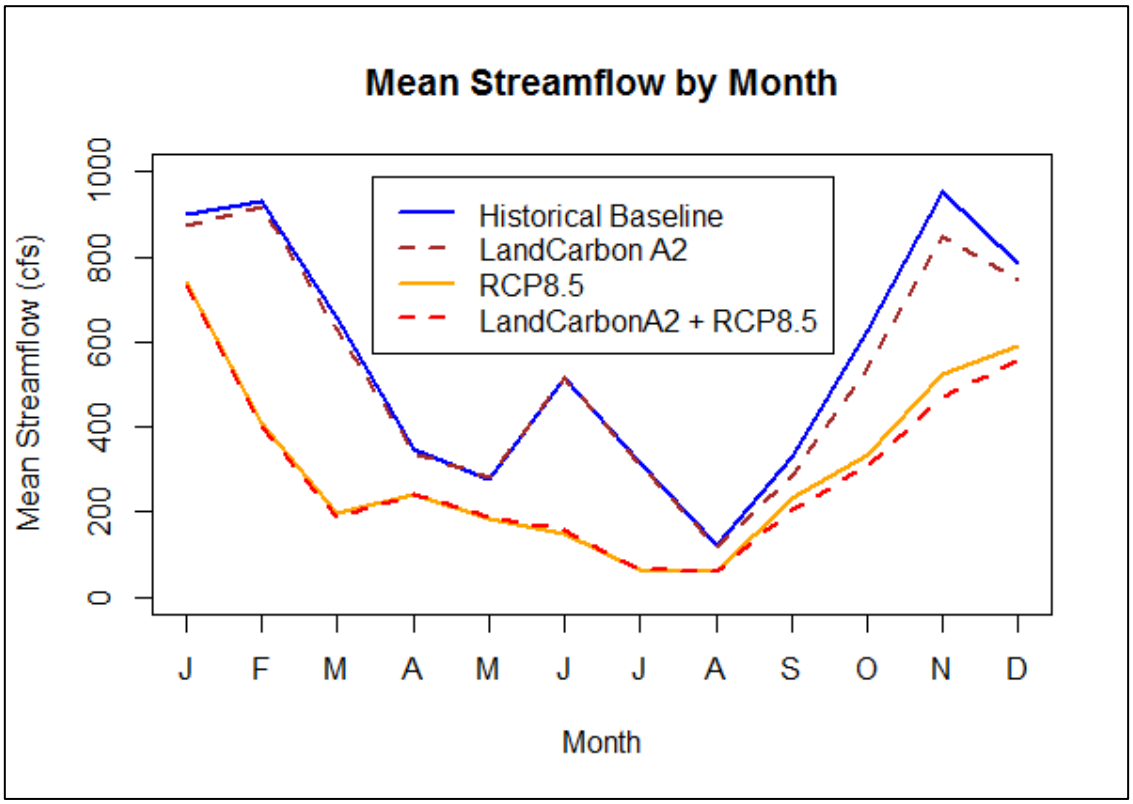

Figure 27. Mean Streamflow by month for each simulation.

Table 29. Mean monthly and annual streamflows for all scenarios and their percent change from the historical baseline simulation.

Month	Historical Baseline	LandCarbon A2		RCP8.5		A2 and RCP8.5	
	Mean Streamflow (cfs)	Mean Streamflow (cfs)	% Change	Mean Streamflow (cfs)	% Change	Mean Streamflow (cfs)	% Change
Jan	1382.21	1281.72	-7.27%	1056.63	-23.56%	1109.54	-19.73%
Feb	1459.62	1362.68	-6.64%	575.92	-60.54%	619.80	-57.54%
Mar	1040.61	993.31	-4.55%	267.52	-74.29%	314.86	-69.74%
Apr	523.68	534.09	1.99%	343.23	-34.46%	439.58	-16.06%
May	436.26	480.89	10.23%	253.60	-41.87%	359.70	-17.55%
Jun	798.10	822.25	3.03%	200.36	-74.90%	280.25	-64.88%
Jul	482.45	523.22	8.45%	76.06	-84.23%	91.58	-81.02%
Aug	176.11	179.00	1.64%	72.30	-58.94%	81.17	-53.91%
Sep	489.49	518.28	5.88%	323.19	-33.98%	362.99	-25.84%
Oct	1002.13	996.78	-0.53%	471.77	-52.92%	490.92	-51.01%
Nov	1552.91	1510.08	-2.76%	774.66	-50.12%	817.09	-47.38%
Dec	1238.70	1160.14	-6.34%	858.10	-30.73%	933.26	-24.66%
Annual	881.86	863.54	-2.08%	439.44	-50.17%	491.73	-44.24%

Table 30. Mean seasonal streamflows for all scenarios and their percent change from the historical baseline simulation.

Season	Historical Baseline	LandCarbon A2		RCP8.5		A2 and RCP8.5	
	Mean Streamflow (cfs)	Mean Streamflow (cfs)	% Change	Mean Streamflow (cfs)	% Change	Mean Streamflow (cfs)	% Change
Winter	1360.18	1268.18	-6.76%	830.22	-38.96%	887.53	-34.75%
Spring	666.85	669.43	0.39%	288.11	-56.79%	371.38	-44.31%
Summer	485.55	508.16	4.66%	116.24	-76.06%	151.00	-68.90%
Fall	1014.85	1008.38	-0.64%	523.21	-48.44%	557.00	-45.12%

4. CONCLUSIONS AND FUTURE RESEARCH

The West Fork San Jacinto River's watershed is expected to undergo rapid urbanization during the coming decades as Houston continues to grow. In addition to this changes to climate threaten the water resources of the region. Lake Conroe, located on the WFSJ River, is a supply reservoir for Houston that will be of growing importance should Houston's population double in size. As the population grows, so too does the demand for water. Climate change increases uncertainty in future water supplies and changes in land use/land cover only serves to exacerbate those uncertainties.

This study evaluated the West Fork San Jacinto River by investigating trends in historical streamflows, changes in LULC, and future scenarios for both climate and LULC. The historical streamflow objectives were achieved by using approaches that feature seasonal trend decomposition, flow distribution, daily streamflow variation, and high flow frequency in conjunction with historical streamflow data. While STL decomposition identified significant downward trends in streamflow, the only significant trend identified was that of monthly mean streamflows.

Changes in LULC were achieved by utilizing NLCD data from the period of 1992-2011. It was found that urban and agricultural land cover has increased while the greatest losses were observed from forested land. These changes in LULC may prove problematic if changes in LULC continue towards this as agriculture and municipal supply are traditionally the greatest consumers of water.

To achieve the goal of investigating future changes in LULC and climate, the VIC hydrological model was employed alongside scenarios of LULC change and climate

change. Changes to LULC were according to the LandCarbon A2 scenario which saw a fivefold increase in urban landscapes and decreases in forested land. In general, other landscapes remained about the same. Changes to climate were addressed using the RCP8.5 climate scenario that assumes business continues as usual. This climate scenario saw reduced precipitation across more rainfall events. A combined scenario of the LandCarbon A2 and RCP8.5 scenarios were also ran. Historical baseline scenarios were ran for the period of 2001 to 20010 and all future scenarios were modeled for the period of 2080-2089.

Results of the modeling efforts showed that there will be mixed results for streamflow resulting from the changes to landscapes with respect to the historical baseline's meteorological forcings. Future climate change scenarios had a great reduction in streamflow for all months compared to the historical baseline. Between the future scenarios, however, the combined LandCarbon A2 and RCP8.5 scenarios has less of a reduced streamflow due to the increased runoff associated with the urbanization and deforestation.

The results of this study highlight the uncertainty facing the hydrology of the WFSJ watershed as changes in LULC and climate are likely to occur. Reductions in streamflows indicate that there will be less water available for the ever-growing Houston metropolitan area. Thus, it is imperative that water resource managers continue to plan for worst-case scenarios to ensure that there is ample water supply in the warming climate and changing landscape.

Future hydrologic modeling research would find it useful to include additional GCMs to compare and contrast their predictions. Future GCM developments could possibly improve the ability to predict extreme events which would improve combined scenarios of land cover and climate changes.

In addition to this, studying multiple watersheds across the GCP of Texas would be a worthwhile endeavor. The difficulties with modeling watersheds that have large reservoirs makes it worthwhile to study watersheds with and without these reservoirs. Additionally, studying inflows to these watersheds would be of use for preparing the future management of those reservoirs. Modeling reservoirs is a difficult task as there are many natural and human factors that come into play with releasing water. This makes it difficult to predict peak flows as well as base flows, thus it would be a useful endeavor to improve existing models or develop new models for modelling reservoirs to increase the accuracy of outflows and how reservoir operations influence streamflows.

REFERENCES

Ackerley, D., Dommenget, D., 2016. Atmosphere-only GCM (ACCESS1. 0) simulations with prescribed land surface temperatures. Geoscientific Model Development, 9(6).

Adnan, R.M., Yuan, X., Kisi, O., Curtef, V., 2017. Application of Time Series Models for Streamflow Forecasting. Civil and Environmental Research, 9(No. 3).

Aulenbach, B.T., Landers, M.N., Musser, J.W., Painter, J.A., 2017. Effects of impervious area and BMP implementation and design on storm runoff and water quality in eight small watersheds. JAWRA Journal of the American Water Resources Association, 53(2): 382-399.

Baddour, D., 2015. Texas flood damage could top $3 billion for 2015, Houston Chronicle, Houston, Texas.

Baker, D.B., Richards, R.P., Loftus, T.T., Kramer, J.W., 2004. A new flashiness index: characteristics and applications to Midwestern rivers and streams. JAWRA Journal of the American Water Resources Association, 40(2): 503-522.

Balling, R.C., Brazel, S.W., 1987. The impact of rapid urbanization on pan evaporation in Phoenix. Arizona. International Journal of Climatology, 7(6): 593-597.

Bates, B., Kundzewicz, Z., Wu, S., Palutikof, J., 2008. Gaps in knowledge and suggestions for further work. Climate change and water, IPCC Tech. Paper IV, IPCC Secretariat: 133-137.

Biasutti, M., Sobel, A.H., Camargo, S.J., Creyts, T.T., 2012. Projected changes in the physical climate of the Gulf Coast and Caribbean. Climatic change, 112(3-4): 819-845.

Booth, D.B., 2000. Forest cover, impervious-surface area, and the mitigation of urbanization impacts in King County, Washington, University of Washington Department of Civil and Environmental Engineering.

Bowling, L.C., Lettenmaier, D.P., 2010. Modeling the effects of lakes and wetlands on the water balance of Arctic environments. Journal of Hydrometeorology, 11(2): 276-295.

Brekke, L., Thrasher, B., Maurer, E., Pruitt, T., 2013. Downscaled CMIP3 and CMIP5 climate and hydrology projections: Release of downscaled CMIP5 climate projections, comparison with preceding information, and summary of user needs.

US Dept. of the Interior, Bureau of Reclamation, Technical Services Center, Denver.

Brody, S., Blessing, R., Sebastian, A., Bedient, P., 2014. Examining the impact of land use/land cover characteristics on flood losses. Journal of Environmental Planning and Management, 57(8): 1252-1265.

Brody, S.D., Highfield, W.E., Ryu, H.-C., Spanel-Weber, L., 2007a. Examining the relationship between wetland alteration and watershed flooding in Texas and Florida. Natural Hazards, 40(2): 413-428.

Brody, S.D., Zahran, S., Maghelal, P., Grover, H., Highfield, W.E., 2007b. The rising costs of floods: Examining the impact of planning and development decisions on property damage in Florida. Journal of the American Planning Association, 73(3): 330-345.

Broxton, P.D., Zeng, X., Sulla-Menashe, D., Troch, P.A., 2014. A global land cover climatology using MODIS data. Journal of Applied Meteorology and Climatology, 53(6): 1593-1605.

Castillo, C.R., Güneralp, İ., Güneralp, B., 2014. Influence of changes in developed land and precipitation on hydrology of a coastal Texas watershed. Applied Geography, 47: 154-167.

Chang, J.X. et al., 2015. Impact of climate change and human activities on runoff in the Weihe River Basin, China. Quaternary International, 380: 169-179. DOI:10.1016/j.quaint.2014.03.048

Channan, S., Collins, K., Emanuel, W., 2014. Global mosaics of the standard MODIS land cover type data. University of Maryland and the Pacific Northwest National Laboratory, College Park, Maryland, USA, 30.

Chen, H.Y., Tong, S.T.Y., Yang, H., Yang, Y.J., 2015. Simulating the hydrologic impacts of land-cover and climate changes in a semi-arid watershed. Hydrological Sciences Journal-Journal Des Sciences Hydrologiques, 60(10): 1739-1758. DOI:10.1080/02626667.2014.948445

Christensen, N.S., Wood, A.W., Voisin, N., Lettenmaier, D.P., Palmer, R.N., 2004. The effects of climate change on the hydrology and water resources of the Colorado River basin. Climatic Change, 62(1-3): 337-363. DOI:10.1023/B:CLIM.0000013684.13621.1f

Clausen, B., Biggs, B., 2000. Flow variables for ecological studies in temperate streams: groupings based on covariance. Journal of hydrology, 237(3): 184-197.

Cleveland, R.B., Cleveland, W.S., Terpenning, I., 1990. STL: A seasonal-trend decomposition procedure based on loess. Journal of Official Statistics, 6(1): 3.

Demographer, O.o.t.S., 2014. 2014 Population Projections Data. Office of the State Demographer.

Diem, J.E., Hill, T.C., Milligan, R.A., 2018. Diverse multi-decadal changes in streamflow within a rapidly urbanizing region. Journal of Hydrology, 556: 61-71.

Dow, C.L., DeWalle, D.R., 2000. Trends in evaporation and Bowen ratio on urbanizing watersheds in eastern United States. Water Resources Research, 36(7): 1835-1843.

Emanuel, K., 2017. Assessing the present and future probability of Hurricane Harvey's rainfall. Proceedings of the National Academy of Sciences: 201716222.

EROS, U., 2013. LandCarbon Conterminous United States Land-Use/Land-Cover Mosaics 1992-2100. In: United States Geological Survey, E.R.O.a.S.C. (Ed.).

Friedl, M.A. et al., 2010. MODIS Collection 5 global land cover: Algorithm refinements and characterization of new datasets. Remote sensing of Environment, 114(1): 168-182.

Fry, J.A., 2011. Completion of the 2006 national land cover database for the conterminous United States. Photogrammetric engineering and remote sensing, 77(9): 858.

Gao, H., Bohn, T., Podest, E., McDonald, K., Lettenmaier, D., 2011. On the causes of the shrinking of Lake Chad. Environmental Research Letters, 6(3): 034021.

Greenwood, E.A.N., 1992. Deforestation, Revegetation, Water Balance and Climate: An Optimistic Path Through the Plausible, Impracticable and the Controversial, Advances in Bioclimatology 1. Springer Berlin Heidelberg, Berlin, Heidelberg, pp. 89-154. DOI:10.1007/978-3-642-58136-6_4

Hamlet, A.F., Lettenmaier, D.P., 1999. Effects of climate change on hydrology and water resources in the Columbia River basin. Journal of the American Water Resources Association, 35(6): 1597-1623. DOI:10.1111/j.1752-1688.1999.tb04240.x

Hansen, M., DeFries, R., Townshend, J.R., Sohlberg, R., 2000. Global land cover classification at 1 km spatial resolution using a classification tree approach. International journal of remote sensing, 21(6-7): 1331-1364.

Highfield, W.E., Brody, S.D., 2006. Price of permits: Measuring the economic impacts of wetland development on flood damages in Florida. Natural Hazards Review, 7(3): 123-130.

Hoekema, D.J., Jin, X., Sridhar, V., 2010. Climate Change and the Payette River Basin, US Society on Dams, Collaborative Management of Integrated Watersheds, 30th Annual USSD Conference, Sacramento, California, pp. 1053-1067.

Homer, C. et al., 2007. Completion of the 2001 national land cover database for the counterminous United States. Photogrammetric Engineering and Remote Sensing, 73(4): 337.

Homer, C. et al., 2015. Completion of the 2011 National Land Cover Database for the conterminous United States–representing a decade of land cover change information. Photogrammetric Engineering & Remote Sensing, 81(5): 345-354.

Hossain, F. et al., 2015. Local-To-Regional Landscape Drivers of Extreme Weather and Climate: Implications for Water Infrastructure Resilience. Journal of Hydrologic Engineering, 20(7). DOI:10.1061/(asce)he.1943-5584.0001210

Hyndman, D.W., 2014. Impacts of Projected Changes in Climate on Hydrology, Global Environmental Change. Springer, pp. 211-220.

Ingebritsen, S.E., Galloway, D.L., 2014. Coastal subsidence and relative sea level rise. Environmental Research Letters, 9(9): 091002.

Khan, S.D., 2005. Urban development and flooding in Houston Texas, inferences from remote sensing data using neural network technique. Environmental Geology, 47(8): 1120-1127.

Knutson, T.R. et al., 2010. Tropical cyclones and climate change. Nature Geoscience, 3(3): 157-163.

Konrad, C.P., Booth, D.B., 2005. Hydrologic changes in urban streams and their ecological significance, American Fisheries Society Symposium, pp. 157-177.

Lall, U., 1995. Recent advances in nonparametric function estimation: Hydrologic applications. Reviews of Geophysics, 33(S2): 1093-1102.

Legesse, D., Vallet-Coulomb, C., Gasse, F., 2003. Hydrological response of a catchment to climate and land use changes in Tropical Africa: case study South Central Ethiopia. Journal of Hydrology, 275(1): 67-85.

Liang, X., Lettenmaier, D.P., Wood, E.F., Burges, S.J., 1994. A SIMPLE HYDROLOGICALLY BASED MODEL OF LAND-SURFACE WATER AND ENERGY FLUXES FOR GENERAL-CIRCULATION MODELS. Journal of Geophysical Research-Atmospheres, 99(D7): 14415-14428. DOI:10.1029/94jd00483

Liang, X., Wood, E.F., Lettenmaier, D.P., 1996. Surface soil moisture parameterization of the VIC-2L model: Evaluation and modification. Global and Planetary Change, 13(1-4): 195-206. DOI:10.1016/0921-8181(95)00046-1

Liu, W.F. et al., 2015. Impacts of climate change on hydrological processes in the Tibetan Plateau: a case study in the Lhasa River basin. Stochastic Environmental Research and Risk Assessment, 29(7): 1809-1822. DOI:10.1007/s00477-015-1066-9

Liu, Y. et al., 2011. Impacts of land-use and climate changes on hydrologic processes in the Qingyi River watershed, China. Journal of Hydrologic Engineering, 18(11): 1495-1512.

Lohmann, D., NOLTE-HOLUBE, R., Raschke, E., 1996. A large-scale horizontal routing model to be coupled to land surface parametrization schemes. Tellus A, 48(5): 708-721.

Lohmann, D., Raschke, E., Nijssen, B., Lettenmaier, D., 1998. Regional scale hydrology: I. Formulation of the VIC-2L model coupled to a routing model. Hydrological Sciences Journal, 43(1): 131-141.

Mango, L.M., Melesse, A.M., McClain, M.E., Gann, D., Setegn, S., 2011. Land use and climate change impacts on the hydrology of the upper Mara River Basin, Kenya: results of a modeling study to support better resource management. Hydrol. Earth Syst. Sci., 15(7): 2245-2258.

Maurer, E.P., Wood, A.W., Adam, J.C., Lettenmaier, D.P., Nijssen, B., 2002. A long-term hydrologically based dataset of land surface fluxes and states for the conterminous United States. Journal of Climate, 15(22): 3237-3251. DOI:10.1175/1520-0442(2002)015<3237:althbd>2.0.co;2

Meyer, S.C., 2005. Analysis of base flow trends in urban streams, northeastern Illinois, USA. Hydrogeology Journal, 13(5-6): 871-885.

Michener, W.K., Haeuber, R.A., 1998. Flooding: natural and managed disturbances. BioScience, 48(9): 677-680.

Moriasi, D.N. et al., 2007. Model evaluation guidelines for systematic quantification of accuracy in watershed simulations. Transactions of the ASABE, 50(3): 885-900.

Mulholland, P.J. et al., 1997. Effects of climate change on freshwater ecosystems of the south-eastern United States and the Gulf Coast of Mexico. Hydrological Processes, 11(8): 949-970.

Muñoz, L.A., Olivera, F., Giglio, M., Berke, P., 2017. The impact of urbanization on the streamflows and the 100-year floodplain extent of the Sims Bayou in Houston, Texas. International Journal of River Basin Management: 1-9.

Muttiah, R.S., Wurbs, R.A., 2002. Modeling the impacts of climate change on water supply reliabilities. Water International, 27(3): 407-419.

Naz, B.S. et al., 2018. Effects of climate change on streamflow extremes and implications for reservoir inflow in the United States. Journal of Hydrology, 556: 359-370.

Olivera, F., DeFee, B.B., 2007. Urbanization and its effect on runoff in the Whiteoak Bayou watershed, Texas. JAWRA Journal of the American Water Resources Association, 43(1): 170-182.

Pachauri, R.K. et al., 2014. Climate Change 2014: Synthesis Report. Contribution of Working Groups I, II and III to the Fifth Assessment Report of the Intergovernmental Panel on Climate Change.

Pluhowski, E., Spinello, A., 1978. Impact of sewerage systems on stream base flow and ground-water recharge on Long Island, New York. US Geological Survey Journal of Research, 6(2): 263-271.

Poff, N.L. et al., 2016. Sustainable water management under future uncertainty with eco-engineering decision scaling. Nature Climate Change, 6: 25-34. DOI:10.1038/nclimate2765

Price, K., 2011. Effects of watershed topography, soils, land use, and climate on baseflow hydrology in humid regions: A review. Progress in physical geography, 35(4): 465-492.

Reddy, S.M.W. et al., 2015. Industrialized watersheds have elevated risk and limited opportunities to mitigate risk through water trading. Water Resources and Industry, 11: 27-45. DOI:10.1016/j.wri.2015.04.001

Schmidt, J.C., Wilcock, P.R., 2008. Metrics for assessing the downstream effects of dams. Water Resources Research, 44(4).

Shuster, W.D., Bonta, J., Thurston, H., Warnemuende, E., Smith, D., 2005. Impacts of impervious surface on watershed hydrology: A review. Urban Water Journal, 2(4): 263-275.

Solis, R.S. et al., 2012. Volumetric and Sedimentation Survey of Lake Conroe: June - August 2010 Survey, Austin, Texas.

Stuckey, A., 2017. Lake Conroe dam's releases cause flood of lawsuits, Houston Chronicle, Houston, TX.

Van Vuuren, D.P., Carter, T.R., 2014. Climate and socio-economic scenarios for climate change research and assessment: reconciling the new with the old. Climatic Change, 122(3): 415-429.

Van Vuuren, D.P. et al., 2011. The representative concentration pathways: an overview. Climatic change, 109(1-2): 5.

Vogelmann, J.E. et al., 2001. Completion of the 1990s National Land Cover Data Set for the conterminous United States from Landsat Thematic Mapper data and ancillary data sources. Photogrammetric Engineering and Remote Sensing, 67(6).

Yang, G., Bowling, L.C., Cherkauer, K.A., Pijanowski, B.C., Niyogi, D., 2010. Hydroclimatic response of watersheds to urban intensity: an observational and modeling-based analysis for the White River Basin, Indiana. Journal of Hydrometeorology, 11(1): 122-138.

Zhu, L., Quiring, S.M., Guneralp, I., Peacock, W.G., 2015. Variations in tropical cyclone-related discharge in four watersheds near Houston, Texas. Climate Risk Management, 7: 1-10.